NAVAL POSTGRADUATE SCHOOL
Monterey, California

THESIS

INVESTIGATION OF THE EFFECTS OF SOLID ROCKET MOTOR
PROPELLANT COMPOSITION ON PLUME SIGNATURE

By

Clay J. Snaza

June 1994

Thesis Advisor: D.W. Netzer

Approved for public release; distribution is unlimited

94 8 18 168

REPORT DOCUMENT PAGE

1. AGENCY USE ONLY (Leave Blank)	2. REPORT DATE 16 JUNE 1994	3. REPORT TYPE AND DATES COVERED Master's Thesis

4. TITLE AND SUBTITLE
INVESTIGATION OF THE EFFECTS OF SOLID ROCKET MOTOR PROPELLANT COMPOSITION ON PLUME SIGNATURE

5. FUNDING NUMBERS

6. AUTHORS
Snaza, Clay J.

7. PERFORMING ORGANIZATION NAME(S) AND ADDRESS(ES)
Naval Postgraduate School
Monterey, CA 93943-5000

8. PERFORMING ORGANIZATION REPORT NUMBER

9. SPONSORING / MONITORING AGENCY NAME(S) AND ADDRESS(ES)
Air Force Phillips Laboratory, Edwards AFB, CA.

10. SPONSORING / MONITORING AGENCY REPORT NUMBER

11. SUPPLEMENTARY NOTES
The views expressed in this thesis are those of the author and do not reflect the official policy or position of the Department of Defense or the U. S. Government.

12a. DISTRIBUTION / AVAILABILITY STATEMENT
Approved for public release, distribution is unlimited.

12b. DISTRIBUTION CODE
A

13. ABSTRACT (Maximum 200 words)

Three propellants with aluminum/silicon weight percentages of 18/0%, 13.5/4.5%, and 12/6% were fired in a subscale motor to determine if the plume infrared signature could be reduced without a significant loss in specific impulse. Spectral measurements from 2.5 to 5.5 um and thermal measurements from 3.5 to 5.0 um were made. Plume particle size measurements showed that only particles with small diameters (less than 1.93 um) were present with any significant volume. Replacing a portion of the aluminum in a highly metallized solid propellant with silicon was found to eliminate the Al_2O_3 in favor of SiO_2 and $Al_6Si_2O_{13}$, without any change in particulate mass concentration or any large change in particle size distribution. These particulates were found to have significantly lower absorptivity than Al_2O_3. An additional investigation was conducted to determine the particle size distribution at the nozzle entrance. Malvern ensemble scattering, phase-Doppler single particle scattering and laser transmittance measurements made through windows in the combustion chamber at the nozzle entrance indicated that large particles were present (to 250 um). However, most of the mass of the particles was contained in particles with diameters smaller than 5 um. Approximate calculations made with the measured data showed that if 100 um particles are present with the smoke (particles with diameters less than 2 um) they could account for only approximately 10% of the particle volume.

14. SUBJECT TERMS
Solid rocket, Aluminum oxide, Infrared signature, Aluminum/Silicon propellant, Particle size distribution

15. NUMBER OF PAGES
66

16. PRICE CODE

17. SECURITY CLASSIFICATION OF REPORT	18. SECURITY CLASSIFICATION OF THIS PAGE	19. SECURITY CLASSIFICATION OF ABSTRACT	20. LIMITATION OF ABSTRACT
UNCLASSIFIED	UNCLASSIFIED	UNCLASSIFIED	UL

Investigation of the Effects of Solid Rocket Motor Propellant Composition

on Plume Signature

by

Clay J. Snaza
Lieutenant Commander, United States Navy
B.S., Central Washington University, 1983

Submitted in partial fulfillment

of the requirements for the degree of

MASTER OF SCIENCE IN ASTRONAUTICAL ENGINEERING

from the

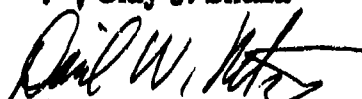**NAVAL POSTGRADUATE SCHOOL**
June 16, 1994

Author: _____
Clay J. Snaza

Approved by: _____
David W. Netzer, Thesis Advisor

_____
Conrad F. Newberry, Second Reader

_____
Daniel J. Collins, Chairman, Department of
Aeronautics and Astronautics

ABSTRACT

Three propellants with aluminum/silicon weight percentages of 18/0%, 13.5/4.5%, and 12/6% were fired in a subscale motor to determine if the plume infrared signature could be reduced without a significant loss in specific impulse. Spectral measurements from 2.5 to 5.5 μm and thermal measurements from 3.5 to 5.0 μm were made. Plume particle size measurements showed that only particles with small diameters (less than 1.93 μm) were present with any significant volume. Replacing a portion of the aluminum in a highly metallized solid propellant with silicon was found to eliminate the Al_2O_3 in favor of SiO_2 and $Al_6Si_2O_{13}$, without any change in particulate mass concentration or any large change in particle size distribution. These particulates were found to have significantly lower absorptivity than Al_2O_3. An additional investigation was conducted to determine the particle size distribution at the nozzle entrance. Malvern ensemble scattering, phase-Doppler single particle scattering and laser transmittance measurements made through windows in the combustion chamber at the nozzle entrance indicated that large particles were present (to 250 μm). However, most of the mass of the particles was contained in particles with diameters smaller than 5 μm. Approximate calculations made with the measured data showed that if 100 μm particles are present with the smoke (particles with diameters less than 2 μm) they could account for only approximately 10% of the particle volume.

iii

TABLE OF CONTENTS

LIST OF TABLES

LIST OF FIGURES

I. INTRODUCTION

Most strategic and many tactical missiles rely on aluminized solid propellants for their propulsion. Composite propellants typically use aluminum as the fuel and ammonium perchlorate (AP) as the oxidizer. These two ingredients combine for roughly 70-90% of the propellant weight. The remainder consists primarily of binder material. The aluminum, usually 14 to 18% of the propellant weight, offers many advantages including: high specific impulse, increased combustion stability, and low cost. A major disadvantage is that during combustion the fuel is oxidized into liquid and solid aluminum oxide which creates a smoky exhaust plume that is also a large source of thermal radiation. [Ref. 1].

Radiation emitted from the plume can be exploited causing a serious decrease in the missiles' lethality. This IR signature can be detected and tracked allowing the target to take evasive action or to counter-target the missile and or the launch platform. As missile technology has advanced the relative size between the vehicle and its plume has decreased. This reduction in radar cross section has precipitated an increased emphasis on IR detection and tracking techniques. As these techniques advance, methods to counter them will increase in importance.

The hot liquid and solid aluminum oxide (Al_2O_3) in the plume is often the main source of radiation. Of this radiation, approximately 90% lies between 0.5 to 5 microns (μm), with peaks between 1 and 2 μm [Ref. 2]. Efforts to accurately predict the plume signature from these propellants have been largely unsuccessful, in part due to the lack of knowledge concerning particle size distribution and temperatures, and the particle optical properties. The latter depend upon particle

1

type and concentration of contamination [Ref. 3]. The phase of the Al_2O_3 particles also has a large effect on their emissivities.

Aluminum oxide melts at 2327 (±6) K. For typical rocket motors the chamber temperature is above this, so the Al_2O_3 is liquid in the chamber [Ref. 2]. As the gas is expanded through the nozzle it can be cooled to below the melting point resulting in liquid and solid particles in the plume. Efforts to determine the optical properties of both liquid and solid Al_2O_3 are ongoing. It has been shown that the emissivity of pure Al_2O_3 is orders of magnitude below that observed from rocket plumes [Ref. 2]. Experiments utilizing carbon and aluminum have shown that a very small percent of absorbing material on the otherwise non-absorbing aluminum oxide enhances the particles emissivity by as much as three orders of magnitude [Ref. 4]. It is generally accepted that the visible and near infrared emission of solid Al_2O_3 is due to impurity type and concentration. For typical propellants and motors the near-field plume thermal radiation is due primarily to liquid Al_2O_3 particles [Ref. 5]. The visible and near-IR emissivity of Al_2O_3 increases drastically upon melting [Ref. 2]. Increases in emissivity by a factor of 40-50 have been reported [Ref. 6]. Until recently it was believed that the emissivity of the liquid, unlike the solid, was not determined by impurities or gas composition. Reference 5 concludes that in the 0.5 to 5 μm range the optical properties of the liquid are controlled by the same processes as the solid. Namely, the type and concentration of contaminates and the details of combustion.

Since the optical properties of both the liquid and solid Al_2O_3 are controlled in part by impurities, it has been suggested that the radiative properties of the exhaust particulates could be tailored for specific applications by coating the particles with thin films [Refs. 2 and 4]. To reduce the IR radiation in solid rocket

2

motor exhaust plumes additives that combine with Al_2O_3 and form particles with favorable optical properties must be cast into the propellant mixture. To be feasible these additives should have no deleterious effect on the propellant performance.

As part of this experiment a study was done to determine possible candidate additives to achieve the desired results of reduced IR plume signature without a significant reduction in specific impulse. Utilizing the Micropep equilibrium combustion code [Ref. 7], computer runs using varying percentages of candidate additives were performed. Starting with a baseline propellant consisting of 73% AP, 12% HTPB, and 15% aluminum, which gave a theoretical specific impulse of 243.9 seconds, the weight percentage of aluminum was varied with the additives. Ratios of 10 to 5, 5 to 10, and 0 to 15% of aluminum to additive were compared. In addition to specific impulse, the products of combustion were compared, as were their optical properties (when they could be found in the literature). The specific impulse results are listed in Table 1. Silicon, magnesium, and calcium performed the best with respect to the least effect on specific impulse. Due to time and cost restraints only one could be used for this investigation. Calcium was eliminated as a choice due to the commercial non-availability of micron sized powder. To decide between magnesium and silicon further study was needed.

TABLE 1. ADDITIVE EFFECTS ON THEORETICAL I_{sp} (sec)

Al/add.	B	C	Ca	Mg	K	Si	Ti	V
10%/5%	241.2	234.5	240.2	242.1	239.4	240.4	239.7	236.4
5%/10%	233.1	212.9	236.2	239.9	232.9	238.9	234.8	229.8
0/15%	227.8	182.5	232.7	239.9	224.1	237.7	229.5	221.1

3

Electrical conductivity and emissivity are connected by Maxwell's equations. Experiments by Reed et al [Ref. 2] showed how the conductivity of a p-type acceptor of (A)-dominated Al_2O_3 was effected after being doped with silicon. As the silicon is added the conductivity initially drops two orders of magnitude to a minimum near 150 ppm and then rises. Their conclusion was that trace impurities can dominate the electrical properties of the particle and hence the optical properties [Ref. 2]. Based on these observations and the previously mentioned effects on specific impulse, silicon was chosen to be the additive for this investigation. These minute traces of silicon would be difficult to add uniformly to a propellant. Even then, it may not be possible to have the silicon "contaminate" the Al_2O_3 vice forming SiO_2 and/or small amounts of $Al_6Si_2O_{13}$. These two species would be the equilibrium products of silicon combustion. Perhaps doping of the aluminum powder could be used. This capability was not available, thus it was decided to instead determine the effect of replacing larger quantities of Al_2O_3 with SiO_2 and $Al_6Si_2O_{13}$ in the plume. It remained to be determined if propellants with reasonable burning rates could be produced using silicon.

In addition to the optical properties, the size distribution of the emitting particles play a significant role in determining plume radiation. The sizes and quantity of particulates in the plume can depend on the particle sizes entering the nozzle and the nozzle geometry. The size distributions can vary in the radial and axial directions throughout the plume. Numerical studies predict that the particle size distribution within the plume is not uniform in the radial direction [Ref. 8]. Particles larger than 5 μm tend to concentrate along the plume centerline, being unable to follow the gas flow as it turns through the throat to the nozzle exit

4

region. For this reason it is expected that the outer region of the plume will be dominated by smaller particles. These particles tend to be at the same temperature as the gas in the exhaust. Temperature decreases through the nozzle of rocket motors and often results in exhaust temperatures below the melting point of Al_2O_3, causing these small particles to be in their solid phase [Ref. 9]. These small solid particles at the outer edge of the plume could have a significant effect on the plume radiance; not only because of the lower emissivity of the solid Al_2O_3, but because the optical properties may be size dependent [Ref. 10]. It was for these reasons that the investigation also included the measurement of plume particle size distribution together with the plume IR signature.

Most of the particle size measurements in this investigation were to be made using a Malvern particle sizer. There has been some question as to the accuracy of these measurements in the rocket motor and plume when the obscuration is very high (greater than 80%) [Ref. 11]. For this reason several auxiliary investigations were conducted as a follow-on to the initial work of Gomes [Ref. 12]. The first utilized a specially formulated propellant with a known size distribution of Al_2O_3 and a flame temperature less than the melting temperature of Al_2O_3. Malvern measurements were then made for comparison with the known distribution. A second investigation utilized a phase-Doppler particle analyzer to make measurements near the chamber wall at the nozzle entrance for comparison with the Malvern measurements across the entire chamber. To further examine the accuracy of the Malvern measurements a laser transmittance measurement through the motor chamber was also made.

5

II. EXPERIMENTAL APPARATUS

A. BACKGROUND

Apparatus for the experiment included: a small solid propellant rocket motor, a Malvern 2600 particle sizing instrument, a AGEMA Thermovision 870 thermal imaging camera, a video camera, a CI Systems SR5000 spectroradiometer, and five different solid propellants. The auxiliary investigation also used a Aerometrics Phase-Doppler Analyzer.

B. EQUIPMENT

1. Propellants

All propellants were provided by the Air Force Phillips Laboratory. The composition of the "calibration" propellants are given in Table 2.

TABLE 2. CALIBRATION PROPELLANT COMPOSITION (WT. %)

	B-183	B-184	B-185
Aluminum Oxide	16.0	16.0	16.0
Ammonium Perchlorate	32.0	32.0	32.0
Ammonium Nitrate	21.9	21.9	21.9
GAP	26.7	26.7	26.7
IPDI	3.2	3.2	3.2
Other	0.2	0.2	0.2
Al_2O_3 size distribution	20% 2 μm 80% 122 μm	65% 2 μm 35% 122 μm	10% 2 μm 70% 5 μm 20% 20 μm

The composition of the propellant used for the Malvern/Phase-Doppler comparison are given in Table 3. Three propellants were used to investigate the

effect of silicon on the plume signature [Table 4]. The control propellant contained 18% aluminum and no silicon. In the other two propellants the aluminum mass concentration was reduced and replaced by an equal mass concentration of silicon, maintaining the metal fuel at a constant 18%. The aluminum/silicon loadings in these two propellants were 13.5% / 4.5% for the first propellant (AC-13) and 12% / 6% for the second (AC-14). These loadings were chosen based on calculations made using the Micropep equilibrium combustion computer code (see Appendix B). Molar concentrations of the major condensed particulates (Al_2O_3, SiO_2, and $Al_6Si_2O_{13}$) in the exhaust varied sharply with concentrations of Al and Si in the propellant [Table 5]. The concentration of $Al_6Si_2O_{13}$ (Mullite) was nearly the same for both propellants and the other compounds were mutually exclusive. The effects of Al_2O_3 and SiO_2 on plume radiation could thus be compared. The mass of the condensed material remained essentially constant.

TABLE 3. MALVERN/PHASE-DOPPLER COMPARISON PROPELLANT

Ingredient	Weight %
Aluminum	2.0
Ammonium Perchlorate	73.0
EG-GAP	14.79
HMDI	0.785
N-100	0.785
TEGDN	8.49
TEPA. No. 3	0.15
$n=0.362$ $c_{th}{}^*=4921$ ft/ser; $\rho_b=0.0629$ lbm/in³ $a=0.06081$	

TABLE 4. AL/SI PROPELLANT COMPOSITION AND PROPERTIES

Propellant	Control	AC-13	AC-14
Ingredients	(wt%)	(wt%)	(wt%)
Aluminum	18.0	13.5	12.0
Silicon	0	4.5	6.0
AP	67.15	67.15	67.15
Dioctyl Adipate	3.91	3.91	3.91
IPDI	0.78	0.78	0.78
R45M	10.14	10.14	10.14
Triphenyl Bismuth	0.02	0.02	0.02
Burning rate exponent Characteristic velocity (ft/s) Burning rate constant	$n=0.378$ $c_{th}*=5148$ $a=0.0195$	$n=0.456$ $c_{th}*=5008$ $a=0.0125$	$n=0.566$ $c_{th}*=4957$ $a=0.0086$
Density (lbm/in^3)	$\rho_b=0.0695$	$\rho_b=0.0627$	$\rho_b=0.0627$

TABLE 5. AL/SI PROPELLANT COMPARISON

Aluminum / Silicon	18% / 0%	13.5% / 4.5%	12% / 6%
Chamber Temp. (K)	3292	3057	2960
Exhaust Temp. (K)	2306	2247	2205
Specific Impulse (s)	244.5	240.6	239.9
Mols Al_2O_3	0.333	0.035	--
Mols SiO_2	--	--	0.036
Mols $Al_6Si_2O_{13}$	--	0.072	0.074
Mols Gas	3.562	3.575	3.585
Mols Condensed	0.333	0.107	0.110
Mol Fraction of Al_2O_3	0.086	0.010	--
Mol Fraction of Condensed	0.086	0.029	0.030
Mass Fraction of Condensed	0.340	0.341	0.330

8

2. Subscale Solid Rocket Motors

A axisymetrical motor 25.4 cm long with a chamber diameter of 5.1 cm was used for the plume signature study. With these motors, radial burning grains were used with a length of 5 cm and a web of 0.63 cm. End burning grains with a burning area of 20.3 cm² were used with a windowed motor for the combustor studies. A nitrogen gas purge system was used to reduce window contamination during the tests with this motor. The motor length provided a residence time of 30-50 ms. Nozzles were constructed out of copper and had a 45° converging half-angle and a 15° diverging half-angle. Nozzle throat and exit diameters were sized to provide approximately ideal expansion from the desired chamber pressure using the following equations:

$$P_c = \left[\frac{A_b}{A_t} c^* \eta_{c^*} a \rho_b \right]^{\frac{1}{1-n}} \qquad \frac{A_e}{A_t} = \frac{1}{M_e} \left[\frac{1 + \frac{\gamma-1}{2} M_e^2}{1 + \frac{\gamma-1}{2}} \right]^{\frac{\gamma+1}{\gamma-1}}$$

$$\frac{P_c}{P_e} = \left[1 + \frac{\gamma-1}{2} M_e^2 \right]^{\frac{\gamma}{\gamma-1}}$$

where

P_c = chamber pressure

P_e = static pressure at the nozzle exit

A_b = propellant burning area

A_t = nozzle throat area

A_e = nozzle exit area

c^* = characteristic velocity for the propellant

η_{c^*} = combustion efficiency

ρ_b = propellant density

a = propellant burning rate constant

9

n = propellant burning rate exponent

M_e = exit Mach number

γ = "process" γ [Ref. 7]

Igniters were constructed of hollowed 1/2 in. bolts filled with $BKNO_3$. Parallel wires inside the bolt were connected by a thin strand of nickel-chromium wire that was resistance heated to ignite the $BKNO_3$. The burning particles produced would spray onto and ignite the surface of the propellant.

3.   Malvern 2600 Particle Sizer

The Malvern 2600 is a non-imaging optical system based on the principle of laser ensemble light scattering employing conventional Fourier optics. Light from a 2 mW Helium-Neon laser at a wavelength of 633 nm is used to form an analyzer beam. Particles passing through this beam cause some of the light to be scattered. The forward scattered light along with the unscattered light are incident onto a receiver lens. This receiver lens operates as a Fourier transform lens, forming the diffraction pattern of the scattered light at its focal plane where a detector is located. The detector is a 31 element solid state photodiode array in the form of a series of concentric semicircular annular rings. This provides 31 separate solid angles of collection. Due to the properties of the range lens the diffraction pattern of a particle within the analyzer beam will remain stationary and centered on the detector regardless of particle position or velocity. The scattered light is collected by the detector, which in turn emits an electronic signal proportional to the light energy. The unscattered light is focused at the centerline where it passes through a small aperture and is recorded on a separate diode. Large particles scatter light at small forward angles and small particles scatter a larger portion of the light at larger angles. For particles over 2 μm in diameter the

10

forward scattered light is largely independent of the optical properties of the material or the suspension medium and is caused mainly by light diffraction around the particle. For particles in the 0.5 to 2 µm range refractive index becomes significant. The Malvern 2600 assumes that the particles are distributed in 32 size bins. Particle size distribution can be displayed as normal, log-normal, Rosin-Rambler, or model independent. Model independent allows measurements of multi-mode distributions. [Ref. 13].

4. SR 5000 Spectroradiometer

Measurements of the spectral emmitance of the rocket motor plume were made with a spectroradiometer. Manufactured by CI systems, the SR5000 measures quantitatively the spectral radiant emittance of objects. To do this it collects radiation from the plume, focuses it on its first focal plane, and chops it at a selectable frequency by using a bladed rotating wheel. This Circular Variable Filter (CVF) wheel covers the range from 2.5 to 14.5 µm. When the chopper obstructs the field of view, it exposes the detector to a reference blackbody. The radiation passes through a field stop to define the field of view, then it is refocused by a mirror onto the detector. The liquid nitrogen cooled indium antimonide detector covers a range from 1.0 to 5.5 µm. The detector outputs an amplified AC signal which, in addition to the reference signal from the chopper, is processed through a synchronous detection circuit. The resulting DC signal is amplified again, digitized, and transferred to the computer for further processing and display. The field of view of the instrument was 5.7°. [Ref. 14]. The combination of the CVF and detector gave a measurement range of 2.5 to 5.5 µm.

5.   IR Camera

The AGEMA 870 Thermovision system was used to measure the radiance of the plume.   The heart of the system is the scanner.   It is thermoelectrically cooled and operates in the short-wave IR band. The scanner converts electromagnetic energy radiated from the object into an electrical signal. The signal from the scanner is amplified and converted into a 12-bit digital signal. The detector within the Thermovision 870 scanner is a strip of Mercury Cadmium Telluride (MCT) mounted on a sapphire substrate. It is sensitive in the range from 2 to 5.6 μm. Thumbwheels on the back of the scanner control the aperture and filter selection. The apertures are selectable so that objects with temperatures from -10°C to +500°C can be measured without filters. The two selectable filters can extend the range to +2000°C. The flame filter is a narrow band-pass type that allows transmittance in the 3.6 to 4.2 μm range. The glass filter acts similarly, allowing radiation from 3.5 to 5.0 μm to be measured. The 870 has seven different scanning modes available.   Using these modes one can select between the highest frame rate, 25 frames per second, or the highest resolution, 280 lines per frame at 6.25 frames per second or other modes in between.   For this experiment the glass filter was used with a frame rate of 25 frames per second. By inputting the emissivity from the emitting surface the system will output data in both temperature (degrees) and radiation (watts/m^2-sr). [Ref. 15].

6.   Phase-Doppler Particle Analyzer

Manufactured by Aerometrics, the Phase-Doppler Particle Analyzer (PDPA) uses a 2 watt argon ion laser with a wavelength of 514.5 nm. A Bragg cell splits the beam into two equal intensity beams separated by 20 mm. One of the beams is phase shifted by 40 MHz, the other is unshifted. The two beams are

passed through a focusing lens which causes the beams to cross at the focal length (250 mm). The volume prescribed by the crossed beams forms the probe volume. Particles passing through this volume scatter light. This scattered light is incident upon a receiver lens located 50^0 above and 238 mm away from the probe volume. The receiver unit directs discrete portions of the scattered light to select photomultiplier tubes (PMTs). The signals from the PMTs are then sent to signal processor. Using high speed analog to digital converters the incoming signals are recorded. A discrete Fourier transform (DFT) along with a fast Fourier transform (FFT) are used to determine the frequency of the signal. [Ref. 16].

The PDPA determines the size of the particle based upon the phase-shift of the scattered light from the particle. In geometric optics, scattered light consists of reflection, refraction, second order refraction, and diffraction. For a specific index of refraction, plots are made of scattered power vs. scattering angles (0-180^0) for each of the individual types of scattering and for the total (Mie) scattering. Angles are chosen where one type of scattering (reflection or refraction) dominates. Then the phase shift at the PMTs produced by a particle passing through the probe-volume is plotted against particle diameter for the chosen type of scattering and scattering angle. This plot is linear for non-absorbing particles when measurements are made of forward scattered refracted light. It is also linear for highly absorbing particles when measurements are made of backscattered reflected light. However, for particles with small diameters (less than 40 μm) and low absorptive index the plot becomes non-linear.

As alluded to in the introduction, the index of refraction and absorption of aluminum oxide varies greatly with temperature, particle size, and impurity type and concentration. The uncertainties in the indexes will translate into

13

III. EXPERIMENTAL CONDITIONS

A. EQUIPMENT LAY OUT AND SEQUENCING

Two separate test configurations were used for the plume signature investigation; one to measure the radiative properties of the plumes and the other to determine the plume particle size distribution. The two layouts are shown in Figure 1. Both layouts included the IR thermal imaging camera looking down on the plume with the same field of view as the spectroradiometer. Comparisons using the radiometric measurements from the IR camera along with chamber pressure data were used to ensure similarity between firings. In order to ensure that the experimental conditions did not differ between firings all runs in configuration (1) [Figure 1(a)] were completed without disturbing the measurement equipment positions or alignment. Then the layout was changed to configuration (2) [Figure 1(b)] and the subsequent runs were completed as before ensuring no equipment disturbance. All the equipment except the video camera were sequenced and triggered by a PC based program named Labtech Notebook. A timing signal was also input into the video recorder from the PC to mark the program start time.

The layouts and sequencing for the auxiliary investigations were slightly different form those discussed above. Because of the extremely high burning rate constant for the calibration propellants ($n \approx .8$) attempts to make measurements during steady-state burning were unsuccessful.

For the investigation to determine particle size distribution within the motor chamber two configuration were needed. Both made use of the windowed

14

motor. The first utilized the PDPA in the configuration shown in Figure 2(a), and the second utilized the Malvern particle sizer as shown in Figure 2(b).

B. PROCEDURE

1. Motor Loading

Propellants were cut into circular shapes to match the motor diameter. If they were to be radial burning they where cut again axially, leaving a 0.63 cm web. They were then inhibited on one face and the sides and bonded to the motor casing. The inhibiting agent was a silicone based self-vulcanizing compound that required 24 hours to cure. After the required curing time the remaining motor components were assembled. Prior to inserting the nozzle, the propellant surface was scratched to ensure an uncontaminated surface for the igniter to impinge on. With the nozzle in place the motor was ready to be mounted to the test stand.

2. Pre-firing

Prior to all firings dry runs were performed to ensure proper sequencing and equipment operation. First the pressure transducer was calibrated using a dead-weight tester. From this information scaling factors were calculated for later use in the data reduction programs to convert transducer voltages into pressure units. With good checks on all equipment the igniter was then installed on the motor and checked for continuity. Then a 12 volt power source was connected to the igniter circuit.

3. Firing

With the igniter connected the motor firing sequence was ready to be started. First, the video recorder was started manually. Next, the Labtech Notebook program was started which in turn immediately initiated the IR camera. The camera was set to record 750 frames at 25 frames per second. The igniter was

manually triggered immediately after the program was started. Once the chamber pressure reached 100 psia the spectroradiometer (or the Malvern particle sizer in configuration (2)) would be triggered. The Malvern was set to take measurements for 30 sweeps requiring approximately 0.24 seconds. The spectroradiometer would take data at 10 scans/second until the buffer was full, approximately 48 scans or 4.8 seconds. Typical burn times averaged one second.

4. Post Firing

At the completion of the run the ignition circuit was deactivated and the video recorder switched off. After allowing the engine to cool, all lenses on the measurement equipment were wiped with alcohol. The motor was then disassembled and cleaned and prepared for the next run. The sequencing and pressure data collected with the Labtech Notebook program were transferred to a spreadsheet program were they could be displayed. Data from the IR camera, spectroradiometer, Malvern 2600, and video camera were recorded separately. The video was reviewed to check for any motor or plume anomalies.

IV. RESULTS AND DISCUSSION

Three separate investigations were conducted with the goal of reducing the infrared emission of a solid rocket motor utilizing an aluminum based propellant, without adversely effecting the specific impulse. First, experiments were performed to determine the accuracy of the Malvern particle sizer. Second, an investigation was conducted to determine the particle size distribution at the nozzle entrance of a solid rocket motor using the Malvern instrument and the phase-Doppler single particle analyzer. Finally, a way to reduce the infrared signature of a solid rocket motor by replacing part of the aluminum fuel with silicon was investigated. Each investigation will be discussed separately below.

A. CALIBRATION PROPELLANTS MEASUREMENTS

This investigation was conducted to determine the accuracy of the Malvern particle sizer in the rocket motor environment when high obscurations are present and/or when the volume distribution is dominated by particles in one size range. Using propellants with known Al_2O_3 particle size distributions (see Table 2) and separate analysis of the Al_2O_3 particles used in the propellant, a comparison was conducted. First, the separate Al_2O_3 particles were suspended in liquid and measured with the Malvern particle sizer. Non-spherical particles with average diameters of 5, 10, 20, and 122 μm were measured. The results of the individual measurements were then combined in the exact ratios as present in the calibration propellants. With these "expected" size distributions known, motor firings with the calibration propellants were attempted in order to make measurements to determine if the particle sizer could distinguish the particle distributions accurately.

17

Eleven motor firings were conducted with the calibration propellants. These propellants proved to be very difficult to ignite. Also, their very high burning rate exponent (n ~ .8), made it difficult to achieve steady-state burning. This made repeatability a problem. The hardest problem to overcome however, was that measurements conducted with the Malvern were often subject to beam steering errors. Beam steering is caused by the thermal gradient present in the motor chamber or the near-field plume; the laser beam is slightly refracted as it passes through the gradient. Its' affects are most pronounced on the small angle detectors, which tended to bias the measurements in favor of the smaller particles. Many techniques to eliminate this problem were attempted with varying degrees of success.

Malvern data are compared to the expected distribution in Figure 3. This was a plume measurement from a firing with a chamber pressure of 120 psia. The modes of the distribution appeared to be properly identified but the mass in modes were not. Beam steering and agglomeration of the particles were possible reasons for the poor correlation.

B. MOTOR CHAMBER MEASUREMENTS

This investigation was conducted to determine particle size distributions within the motor chamber. Utilizing a phase-Doppler single particle analyzer and the Malvern ensemble particle sizer, measurements through a windowed motor were conducted. Measurements from these two devices were compared.

A total of seven motor firings were performed for this investigation; three utilizing the phase-Doppler particle sizer, and four using the Malvern particle sizer. Of the four Malvern runs two were conducted with a modified windowed motor. In addition to the windows, the modified design had tubes with a 1.27 cm

18

diameter inserted in the window cavities on each side leaving a measurement volume with a 1.27 cm length along the centerline of the motor. This reduction in the beam length containing particles was implemented in an attempt to reduce the obscuration caused by the scattering from the smaller particles.

The PDPA was set to measure only the larger particles (5-250 μm) since particles larger than 40-50 μ had not been detected by the Malvern. The data, displayed in Figure 4, shows that a only a small number percentage of the particles in this size range had diameters greater than 10 μm. But they made up a large percent of the volume. In fact, for all three firings the Sauter mean diameter (D_{32}) was relatively constant at 214 μm. Of course the PDPA neglected the mass of all particles with diameters smaller than 5 μm. Most of the particles present in the motor chamber are believed to have diameters less than 5 μm. The instrument cannot, therefore, give the percent of mass in the measured range even at the local measurement point.

Two firings were made with the Malvern and the unmodified windowed motor. The Malvern data is shown in Figure 5. A pressure-time trace with Malvern data acquisition times are shown in Figure 6. Two runs were conducted with very similar results. In both runs the obscuration was approximately 96% and D_{32} = 2.95 μm (the smallest that could be measured with the 300 mm lens). The Malvern did not measure any particles larger than 5.80 μm. In the second test a second measurement was made during the burning tailoff. Here again, the obscuration was high (approximately 99%), but all of the particle volume was in diameters greater than 34 μm (D_{32} = 70 μm, number mode = 44 μm) [Figure 7]. Thus, it appears that the Malvern can detect large particles in flows with high obscurations. In the plume tailoff many of the smaller particles apparently exit the

19

nozzle but the larger particles continue to circulate with the window purge gas. In addition, larger particles are probably formed on the remaining propellant surface. To investigate this further a modified motor was fabricated in an attempt to reduce the obscuration during the Malvern measurements.

The Malvern data obtained with the modified motor are shown in Figure 8. Once again the obscuration was very high (approximately 99%) and the average particle size measured was the minimum value of $D_{32} = 2.95\ \mu m$. Thus, the Malvern could not detect the larger particles (observed in the tailoff and by the PDPA) in the presence of many small particles during the steady-state burning. Measurements made in the tailoff region [Figure 9] were similar to those obtained with the unmodified motor, i.e. larger particles were measured. The question to be answered was what mass (volume) fraction of the particles is contained in the larger (greater than 5 μm) sizes during the steady burn.

An analysis was conducted to determine the percentage of large particles possible with this high obscuration. The following transmittance equation was used [Ref. 17]:

$$T_r = e^{-\frac{3L}{2D_{32}}\overline{Q}C_v}$$

where: T_r = fraction of light transmitted

L = path length

$\overline{Q}$ = mean extinction coefficient

D_{32} = volume-to-surface mean (Sauter) particle diameter

C_v = volume concentration of particles

The above equation can be solved for D_{32}. C_v is calculated based upon the propellant composition and assumes that all aluminum is burned to form Al_2O_3. Setting $T_r = .04$ (obscuration = .96), $L = 5$ cm (the unmodified motor), $\overline{Q} = 2$

20

(average for particle diameters greater than 5 μm) and solving yields 2.1 μm for D_{32}. If the assumption is made that all the particles are either 2.1 μm or 100 μm one can determine the percentage of the large (100 μm) particles needed to produce the measured obscuration of 96%. Since

$$D_{32} = \frac{N_{2.1}(2.1)^3 + N_{100}(100)^3}{N_{2.1}(2.1)^2 + N_{100}(100)^2} = 2.1 \mu m$$

where: $N_{2.1}$ = number of particles with diameters = 2.1 μm

           N_{100} = number of particles with diameters = 100 μm

$N_{2.1}$ = (979000)N_{100}. The volume percentage of large particles is:

$$\frac{Vol_{100}}{Vol_{100} + Vol_{2.1}} = \frac{N_{100}(100)^3}{N_{100}(100)^3 + N_{2.1}(2.1)^3}$$

with $N_{2.1}$ = (979000)N_{100};

$$\frac{Vol_{100}}{Vol_{100} + Vol_{2.1}} = 0.093$$

This shows that only 9.3% of the particle mass could be in the 100 μm particles in order to produce an obscuration of 96% (or transmittance of 4%). Similar calculations were performed with D = 0.496 μm and $\bar{Q}$ = 4.78 (from a Mie code). This yielded a D_{32} of 5.00 μm and a 100 μm diameter volume percent possible of 9.5%. These calculations show that the maximum percent by volume of large particles ((~ 100 μm) that could be present with an obscuration at 96% is less than 10% of the total volume. It appears then, that the obscuration seen with the Malvern particle sizer is caused by the high percentage of small particles.

A small amount of beam steering could give a false value of high obscuration by the Malvern. For this reason a separate experiment was conducted to determine the transmittance through the windowed motor during a motor burn. To accomplish this, a helium-neon laser beam was passed through the windows of the

21

motor during a firing and its intensity was recorded. This was accomplished using the modified motor with tubes inserted into the window cavities to help ensure that the windows would remain uncontaminated. The results are shown in Figure 10. A percent reduction in transmittance was calculated from this data . For a 1.27 cm beam length the transmittance was 56%. For a beam length of 5.0 cm the transmittance would be approximately 10%. This was close to the 96 to 99% obscuration measured with the Malvern instrument The additional 6 to 9% measured with the Malvern was probably due to beam steering. So it appears that the majority of the obscuration is caused by the smaller particles. This supports the assumption made above, i.e. that the majority of the particles and particle mass in the motor chamber are small (much less than 100 μm).

C. PLUME RADIATION MEASUREMENTS

A propellant containing 18% aluminum was modified by replacing part of the aluminum with silicon. It was hoped that the silicon would combine with the aluminum and either reduce or eliminate the Al_2O_3 particles in the plume and replace them with particles that would have more favorable optical properties; that is, particles that emit less radiation in the infrared region and thereby reduce the overall emittance of the plume.

Measurements were collected from the three propellants previously mentioned: 18% aluminum, 12%/6% aluminum/silicon, and 13.5%/4.5% aluminum/silicon. Radiation and spectral measurements were taken of the same area of each plume. In addition, Malvern particle size distribution measurements were collected from the plumes at the same distance from the nozzle.

Initial tests with end-burning grains produced very progressive pressure-time traces due to nozzle clogging. This was due to the high aluminum loading in the

propellant and the small nozzle throat areas. Utilizing a radial burning grain and a larger nozzle throat area resulted in a less progressive burn [Figure 11]. All subsequent tests with the 18% aluminum as well as the propellants modified with silicon were conducted with radial burning grains.

All propellants had similar burning rates so the same motor and nozzle combination was used for all runs. The nozzle throat diameter was 0.69 cm with an exit diameter of 1.27 cm. This configuration provided neutral burning patterns for the aluminum/silicon propellants with peak pressure near 400 psia [Figures 12 and 13]. All comparisons between the propellants were made at or very near 400 psia and with nearly ideal expansion (p_e=26 psia). Individual propellant results are discussed below.

1. **Plume Particles Size Measurements**

    The Malvern particle sizer was positioned 6.1 nozzle exit diameters aft of the nozzle exit. Beam steering and detector saturation were anticipated due to the high thermal gradients seen during the earlier firings. A wide-pass laser line filter was installed on the receiver lens in order to reduce the chance of saturation. The Malvern was triggered to record 30 sweeps when the chamber pressure reached 100 psia. Particle size measurements for the 18% propellant were acquired from a low pressure burn (approximately 140 psia) and are shown in Figure 19. Previous experiments have shown that larger particles are more prevalent in the plumes when the chamber pressure is low. This leads one to believe that if this propellant were run at a pressure of 400 psia, like the other propellant, the particles would have been even smaller. Of the three propellants only the 18% Al showed any particles with diameters greater than 1.93 μm. Even in this case 90% of the particle volume was in the particles smaller than 1.93 μm in diameter and the

23

maximum size was less than 5.5 μm. Malvern measurements for the two aluminum/silicon propellants are shown in Figures 20 and 21. Both of the silicon enhanced propellants appeared to have only small (less than 1.93 μm) particles in their exhaust plumes.

2. Thermal comparison

All runs with the 18% aluminum propellant produced progressive pressure-time traces [Figure 11]. This propellant was used as a base-line to which the aluminum/silicon propellants could be compared. Thermal images from the three propellants are shown in Figures 14 through 16. An area box was used to determine the average radiance and total power from the area of the plume that was viewed by both the AGEMA IR camera and the spectroradiometer. Table 6 lists the average radiance and total power as well as the peak temperature (for an emissivity of 0.18) in the plume. These data were obtained from the average of five sequential images.

TABLE 6. PLUME THERMAL COMPARISON

Propellant	AC7 5/27	AC7 5/31	AC13 6/1	AC14 6/3	AC14 6/4
Ave. Pressure (psia)	401	401	408	402	425
Total Power (W)*	71.7	65.6	75.8	85.4	80.9
Radiance (W/ಟಡ² sr)	1320	1450	1500	1710	1600
Max. Temp.(°C)	941	929	934	1251**	922

* measurement area = 0.14 m²

** due to local Mach disk

Table 6 shows that as the silicon was increased (Al decreased) the radiation also increased (by approximately 20%). In order to determine whether

24

the radiation was caused by the gas or the condensed particles, the spectrum of the plume needs to be examined.

3. Radiometric Measurements

The spectroradiometer measures the spectral range from 2.5 to 5.5 μm. Placed at a distance of 5 meters from the motor with a 5.7 degree lens the spectroradiometer provided approximately a 0.5 m field of view. The instrument was triggered to begin recording at a chamber pressure equal to 100 psia. Spectral measurements from the three propellants are shown together in Figure 17. These three spectrums were obtained with pressures between 402 and 425 psia. To determine whether the observed variations could have been caused by pressure differences a comparison of the 18% propellant spectrum obtained at 400 psia and at 450 psia are shown in Figure 18. This shows that the spectrum is only slightly sensitive to variances in pressure and the differences in the three spectrums measured were caused by plume characteristics and not pressure differences. As can be seen from the figure the plume does not strongly radiate as a continuum, as would be the case if the particles were producing the radiation. The plume radiation spectrum was dominated by the CO and H_2O gases in the exhaust. As the silicon loading was increased at the expense of aluminum the radiation in the CO and H_2O bands increased. This occurred even with a slight reduction in the equilibrium number of moles of CO and H_2O (approximately constant mole fraction) in the plume. The increase in radiation was also in agreement with the observed behavior from the thermal imaging camera. The equilibrium concentration of CO remained approximately constant and the concentration of H_2 increased slightly. Thus, there could have been a slight increase in afterburning which could, in turn, increase the CO plus H_2O radiation. Since no significant

25

change in plume maximum temperature or plume temperature profile occurred, it indicated that increased afterburning did not occur. The plume particle sizes from these propellants were very similar and small. In addition, the equilibrium calculations indicated that the particulate mass remained constant. These results from the combined spectral, thermal imaging and particle sizing measurements together with the equilibrium calculations indicate that the particles acted primarily as scatterers of radiation rather than as emitters. They also imply that the SiO_2 and $Al_6Si_2O_{13}$ particles absorb less radiation from the gas than does Al_2O_3, indicating that they have a lower absorbtivity (emissivity). At low altitudes where strong afterburning can occur this change in emissivity may not be as significant as at high altitudes, where the particle radiation can dominate the plume IR signature.

V. CONCLUSIONS

Malvern ensemble scattering, phase Doppler single particle scattering, and laser transmittance measurements made through windows in the combustion chamber at the nozzle entrance indicated that large particles were present (to 250 μm). However, most of the mass of the particles was contained in particles with diameters smaller than 5 μm. Approximate calculations made with the measured data showed that if 100 μm particles are present with the smoke (particles with diameters less than 2 μm) they could account for only approximately 10% of the particle volume.

Replacing a portion of the aluminum in a highly metallized solid propellant with silicon was found to eliminate the Al_2O_3 in favor of SiO_2 and $Al_6Si_2O_{13}$, without and change in particulate mass concentration or any large change in particle size distribution. These particulates were found to have significantly lower absorptivity than Al_2O_3.

APPENDIX A

FIGURES
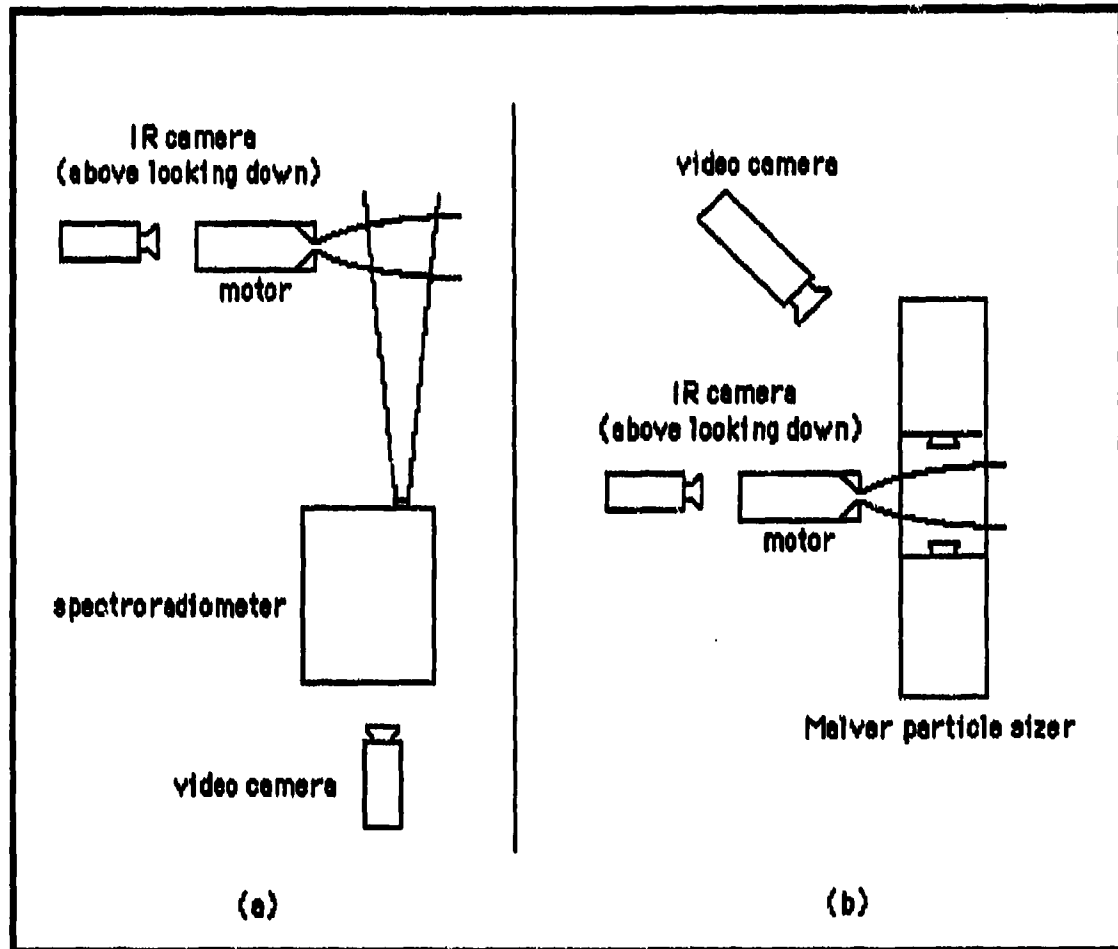
Figure 1. Plume Radiation Measurement Layout
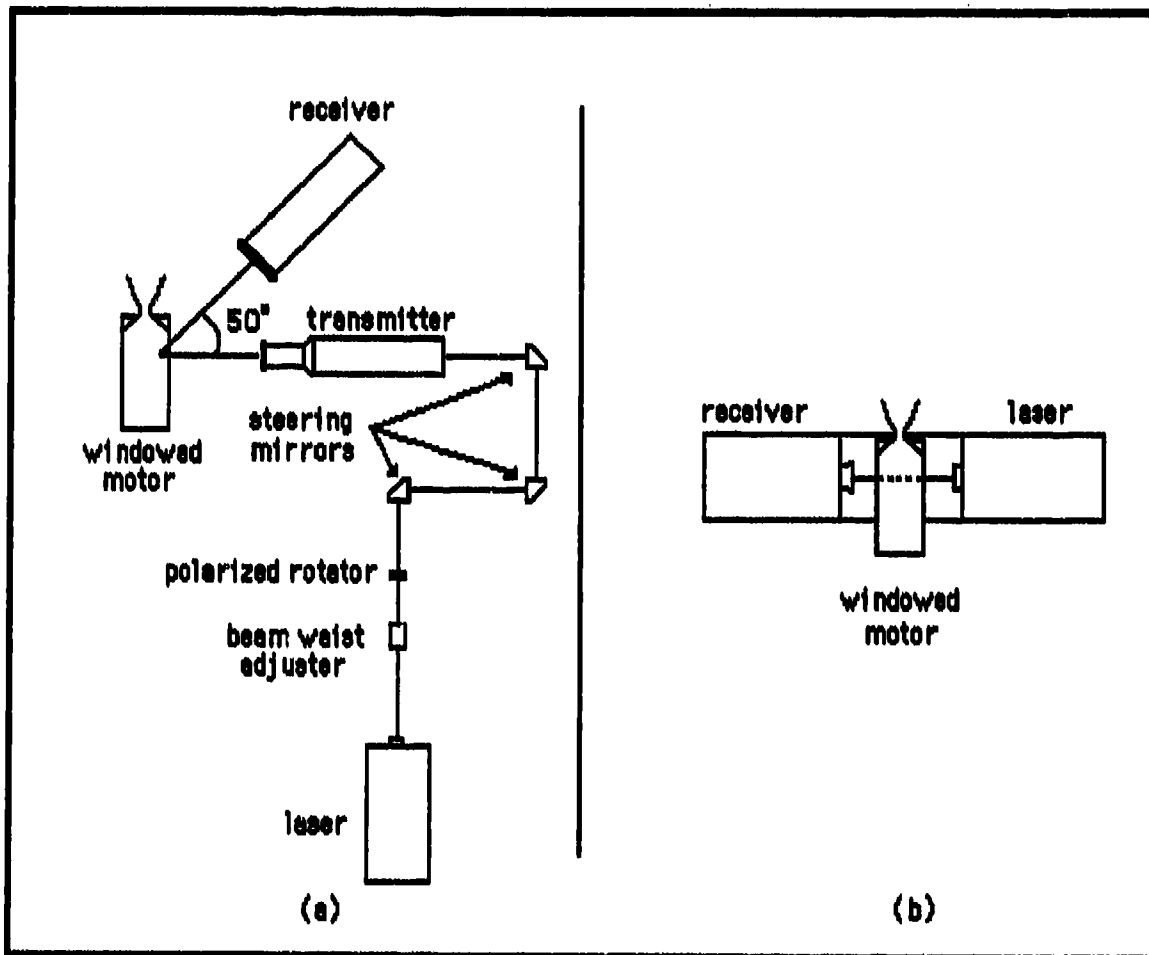
Figure 2. PDPA/Malvern Through Motor Measurement Layout

29

B-185 4-14-94 malv.rec.#141(___) vs. Predicted (_ _)
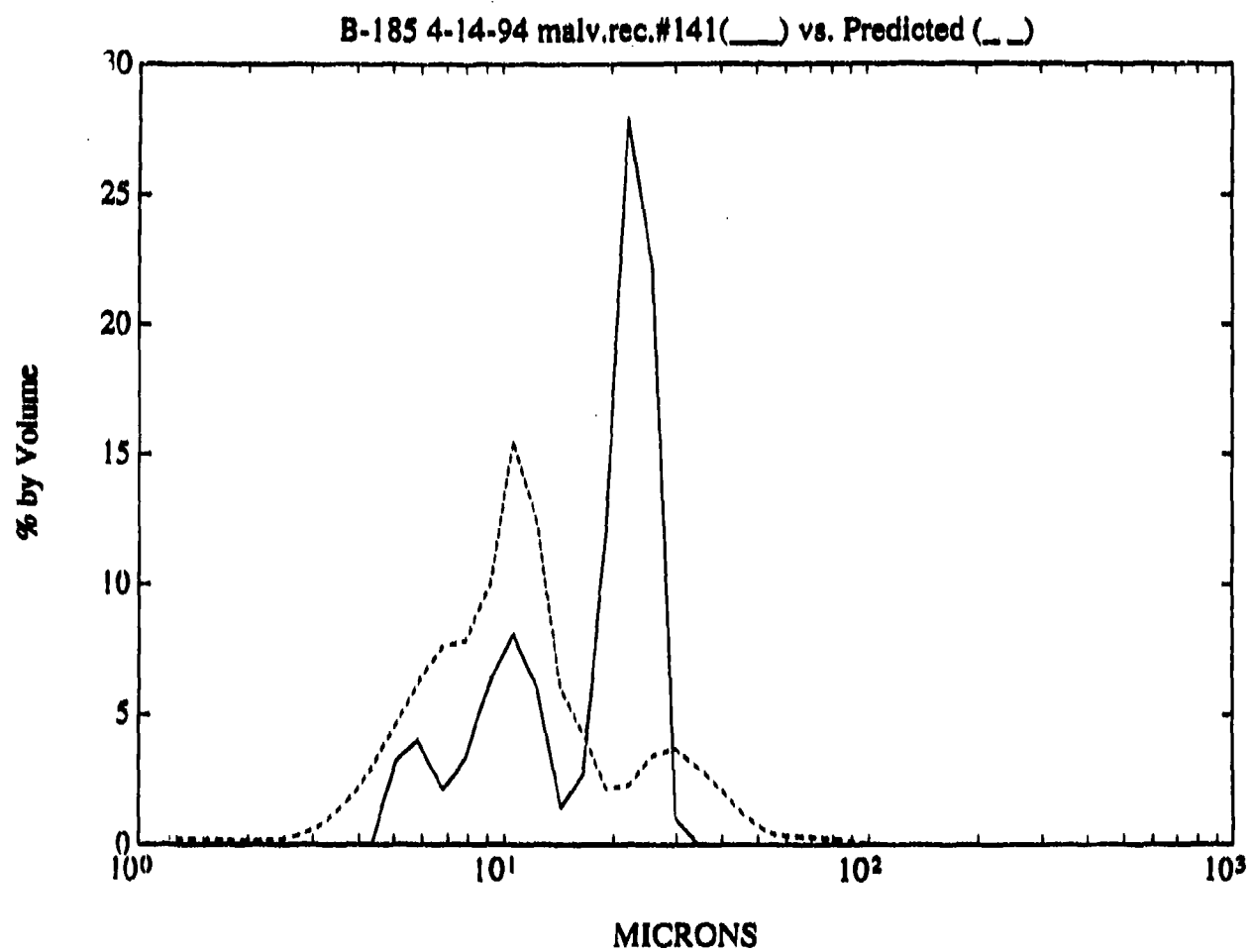
Figure 3. Calibration Propellant Comparison to Predicted

30

Arithmetic Mean (D10) = 94.8 um
Area Mean (D20) = 134.9 um
Volume Mean (D30) = 156.9 um
Sauter Mean (D32) = 212.3 um

	Ch1	Ch2	Ch3
Attempts	3252		
Valid	155		
% Valid	5		
Corrected			
Run Time	17.63 sec		

CH1 Velocity Mean = 2.559 m/s
RMS = 2.873 m/s
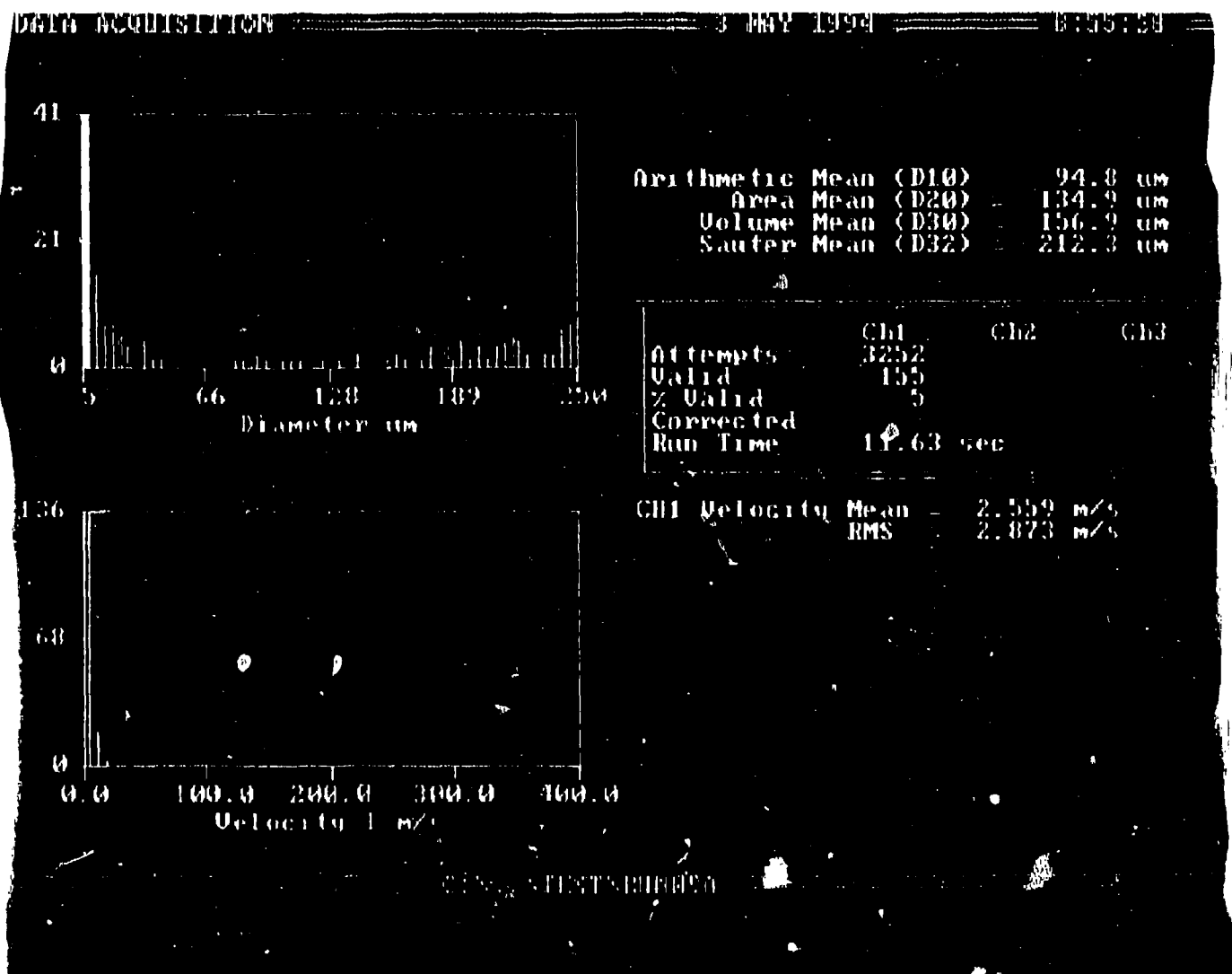
Figure 4. PDPA Motor Chamber Results

31

Upper	in	Lower	Under	Upper	in	Lower	Under	Upper	in	Lower	Under	Span 0.85
				173	0.0	150	100	29.5	0.0	25.4	100	
				150	0.0	129	100	25.4	0.0	21.9	100	D[4,3]
				129	0.0	111	100	21.9	0.0	18.9	100	2.95µm
				111	0.0	96.0	100	18.9	0.0	16.3	100	
564	0.0	487	100	96.0	0.0	82.5	100	16.3	0.0	14.1	100	D[3,2]
487	0.0	420	100	82.5	0.0	71.5	100	14.1	0.0	12.1	100	2.95µm
420	0.0	362	100	71.5	0.0	61.5	100	12.1	0.0	10.4	100	
362	0.0	313	100	61.5	0.0	53.0	100	10.4	0.0	9.05	100	D[v,0.9]
313	0.0	270	100	53.0	0.0	45.8	100	9.05	0.0	7.80	100	4.49µm
270	0.0	233	100	45.8	0.0	39.5	100	7.80	0.0	6.70	100	
233	0.0	201	100	39.5	0.0	34.1	100	6.70	0.0	5.80	100	D[v,0.1]
201	0.0	173	100	34.1	0.0	29.5	100	5.80	100	1.50	0.0	1.96µm

Source = Dataiclay	Beam length = 40.0 mm	Model indp
Record No. = 164	Log. Diff. = 4.782	
Focal length = 300 mm	Obscuration = 0.9631	Volume Conc. = 0.0081%
Presentation = pia	Volume distribution	Sp.S.A 2.0339 m²/cc.

D[v,0.5] 2.96µm

Shape OFF

2048 pia ldr487 / 0/ 0/0.00/1.00/
AC-11, through the motor, dthrt=.21"   300mm lens,30 sweeps x 8 loops ,laser
line filter   000001113
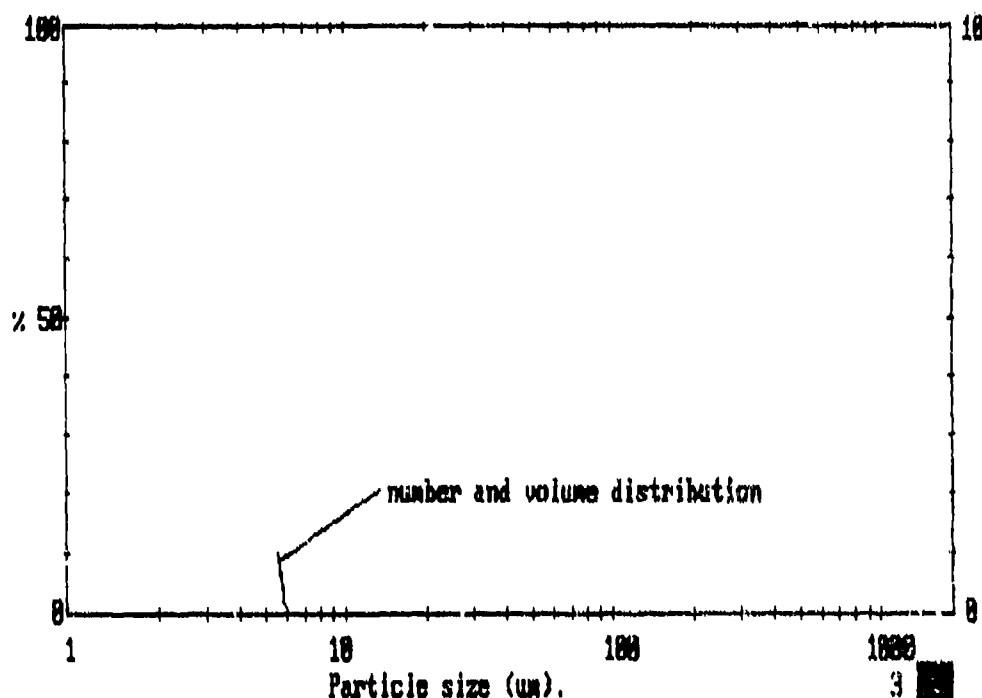
2048 pia ldr487 / 0/ 0/0.00/1.00/
AC-11, through the motor, dthrt=.21"   300mm lens,30 sweeps x 8 loops ,laser
line filter   000001113

Figure 5. Malvern Motor Chamber Results

AC-11 5-4-94

malvern thru motor
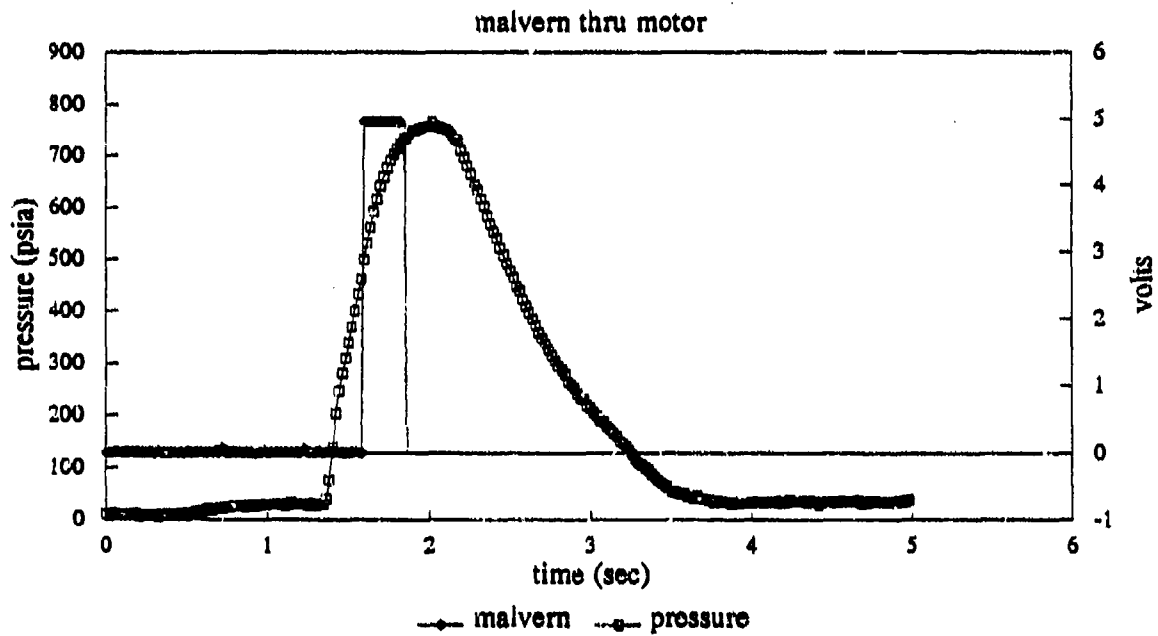
Figure 6. Malvern Data Acquisition Time and Pressure Time Trace

33

MALVERN   Series 2b00   SB.OD   Master Mode   04 May 1994   9:01 am

Upper	In	Lower	Under	Upper	In	Lower	Under	Upper	In	Lower	Under	Span
				173	0.5	150	99.5	29.5	0.0	25.4	0.0	0.80
				150	3.0	129	96.5	25.4	0.0	21.9	0.0	D[4,3]
				129	5.2	111	91.3	21.9	0.0	18.9	0.0	78.01μm
				111	16.2	96.0	75.0	18.9	0.0	16.3	0.0	
564	0.0	487	100	96.0	20.1	82.5	54.9	16.3	0.0	14.1	0.0	D[3,2]
487	0.0	420	100	82.5	11.2	71.5	43.7	14.1	0.0	12.1	0.0	69.75μm
420	0.0	362	100	71.5	10.0	61.5	33.6	12.1	0.0	10.4	0.0	
362	0.0	313	100	61.5	12.5	53.0	21.1	10.4	0.0	9.05	0.0	D[v,0.9]
313	0.0	270	100	53.0	11.6	45.8	9.5	9.05	0.0	7.80	0.0	108.85μm
270	0.0	233	100	45.8	7.9	39.5	1.7	7.80	0.0	6.70	0.0	
233	0.0	201	100	39.5	1.7	34.1	0.0	6.70	0.0	5.80	0.0	D[v,0.1]
201	0.0	173	100	34.1	0.0	29.5	0.0	5.80	0.0	1.59	0.0	46.16μm

Source = Dataiclay	Beam length = 40.0 mm	Model indp	D[v,0.5]
Record No. = 165	Log. Diff. = 5.993		77.96μm
Focal length = 300 mm	Obscuration = 0.9900	Volume Conc. = 0.2679%	
Presentation = pia	Volume distribution	Sp.S.A 0.0860 m²/cc.	Shape OFF

2048 pia ldr487 / 0/ 0/0.00/1.00/
AC-11, through the motor, dthrt=.21"   300mm lens,30 sweeps x 8 loops ,laser
line filter   000001114

MALVERN   Series 2600   SB.OD   Master Mode   04 May 1994   9:01 am

2048 pia ldr487 / 0/ 0/0.00/1.00/
AC-11, through the motor, dthrt=.21"   300mm lens,30 sweeps x 8 loops ,laser
line filter   000001114
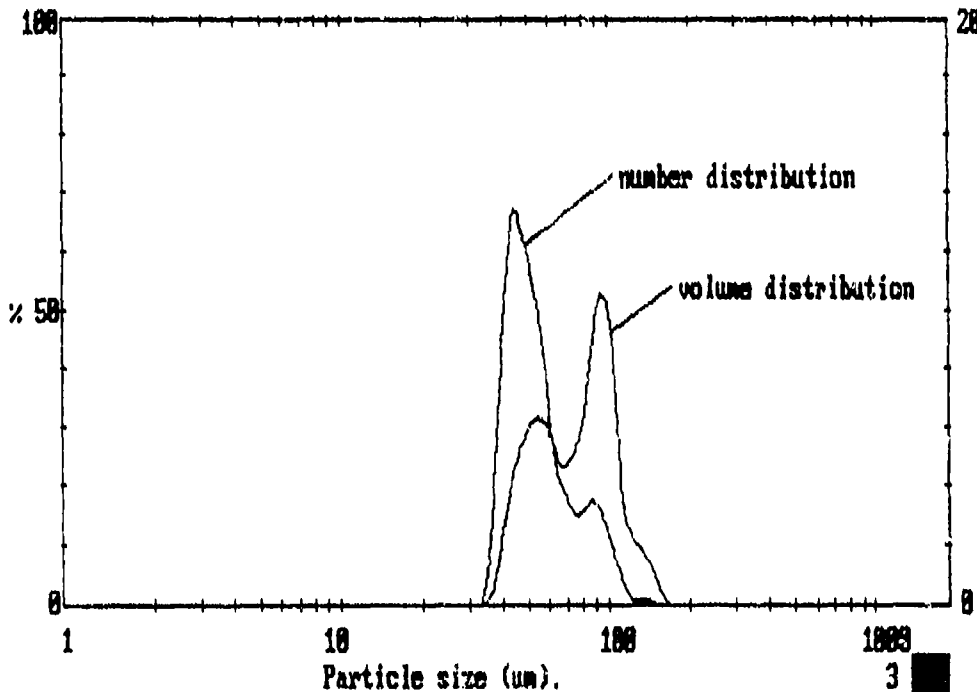
Figure 7. Malvern Measurement: Through Motor During Burn Tailoff

34

Upper	in	Lower	Under	Upper	in	Lower	Under	Upper	in	Lower	Under	Span
												0.85
				173	0.0	150	100	29.5	0.0	25.4	100	
				150	0.0	129	100	25.4	0.0	21.9	100	D[4,3]
				129	0.0	111	100	21.9	0.0	18.9	100	2.95µm
				111	0.0	96.0	100	18.9	0.0	16.3	100	
564	0.0	487	100	96.0	0.0	82.5	100	16.3	0.0	14.1	100	D[3,2]
487	0.0	420	100	82.5	0.0	71.5	100	14.1	0.0	12.1	100	2.95µm
420	0.0	362	100	71.5	0.0	61.5	100	12.1	0.0	10.4	100	
362	0.0	313	100	61.5	0.0	53.0	100	10.4	0.0	9.05	100	D(v,0.9)
313	0.0	270	100	53.0	0.0	45.8	100	9.05	0.0	7.80	100	4.49µm
270	0.0	233	100	45.8	0.0	39.5	100	7.80	0.0	6.70	100	
233	0.0	201	100	39.5	0.0	34.1	100	6.70	0.0	5.80	100	D(v,0.1)
201	0.0	173	100	34.1	0.0	29.5	100	5.80	100	1.50	0.0	1.96µm

Source = Dataclay	Beam length = 40.0 mm	Model indp	D(v,0.5)
Record No. = 131	Log. Diff. = 4.702		2.96µm
Focal length = 300 mm	Obscuration = 0.9900	Volume Conc. = 0.0113%	
Presentation = pia	Volume distribution	Sp.S.A 2.0339 m²/cc.	Shape OFF

2048 pia ldr487 / 3/ 0/0.00/1.00/
AC-11,Malvern with tubes, dthrt=.24", 300mm lens, 30sweeps x2loops

000001119

number and volume distribution

Particle size (um).

2048 pia ldr487 / 3/ 0/0.00/1.00/
AC-11,Malvern with tubes, dthrt=.24", 300mm lens, 30sweeps x2loops

000001119

Figure 8. Malvern Measurement: Modified Motor

MALVERN   Series 2600   SB.0D   Master Mode   09 May 1994   9:28 am

Upper	in	Lower	Under	Upper	in	Lower	Under	Upper	in	Lower	Under	Span 7.37
				173	0.0	150	100	29.5	3.0	25.4	80.7	
				150	0.0	129	100	25.4	0.6	21.9	80.1	D[4,3]
				129	0.0	111	100	21.9	0.5	18.9	79.5	9.56µm
				111	0.0	96.0	100	18.9	0.5	16.3	79.1	
564	0.0	487	100	96.0	0.0	82.5	100	16.3	0.4	14.1	78.7	D[3,2]
487	0.0	420	100	82.5	0.0	71.5	100	14.1	0.4	12.1	78.3	3.96µm
420	0.0	362	100	71.5	0.0	61.5	100	12.1	0.4	10.4	77.9	
362	0.0	313	100	61.5	0.0	53.0	100	10.4	0.6	9.05	77.3	D[v,0.9]
313	0.0	270	100	53.0	0.0	45.8	100	9.05	1.1	7.80	76.2	33.03µm
270	0.0	233	100	45.8	0.0	39.5	100	7.80	3.0	6.70	73.2	
233	0.0	201	100	39.5	7.7	34.1	92.3	6.70	5.1	5.80	68.1	D[v,0.1]
201	0.0	173	100	34.1	8.6	29.5	83.7	5.80	68.1	1.50	0.0	2.20µm

Source = Data:clay	Beam length = 40.0 mm	Model indp
Record No. = 182	Log. Diff. = 3.770	
Focal length = 300 mm	Obscuration = 0.9900	Volume Conc. = 0.0152%
Presentation = pia	Volume distribution	Sp.S.A 1.5164 m²/cc.

D[v,0.5] 4.18µm

Shape OFF

2048 pia ldr487 / 3/ 0/0.00/1.00/
AC-11,Malvern with tubes, dthrt=.24", 300mm lens, 30sweeps x2loops

000001120

MALVERN   Series 2600   SB.0D   Master Mode   09 May 1994   9:28 am
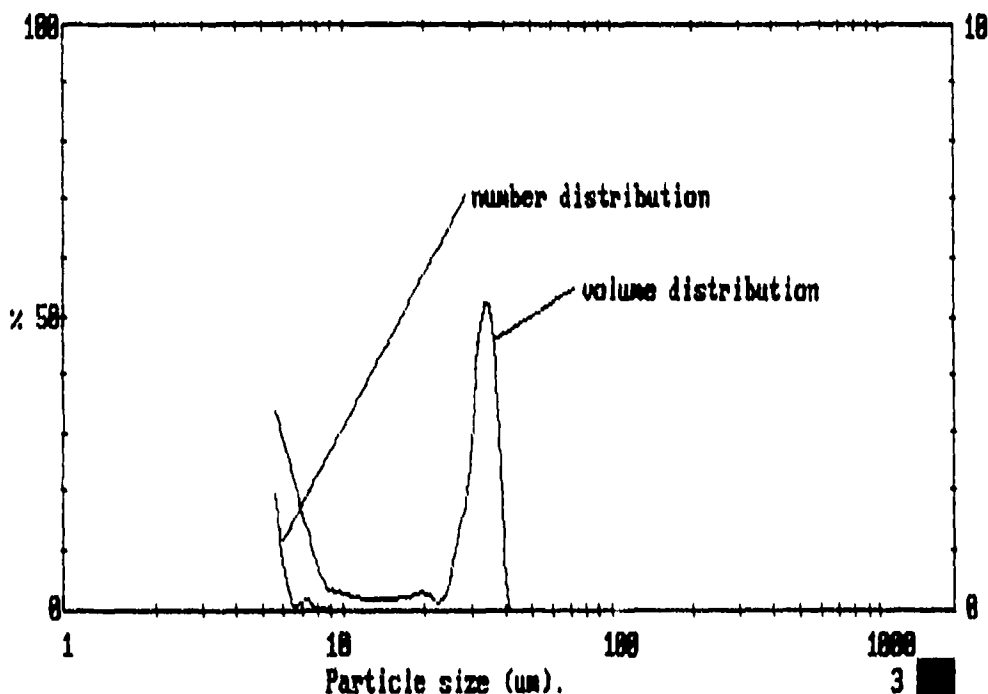
2048 pia ldr487 / 3/ 0/0.00/1.00/
AC-11,Malvern with tubes, dthrt=.24", 300mm lens, 30sweeps x2loops

000001120

Figure 9. Malvern Measurement: Modified Motor During Burn Tailoff

3 6

AC-11 5-30-94

transmittance test
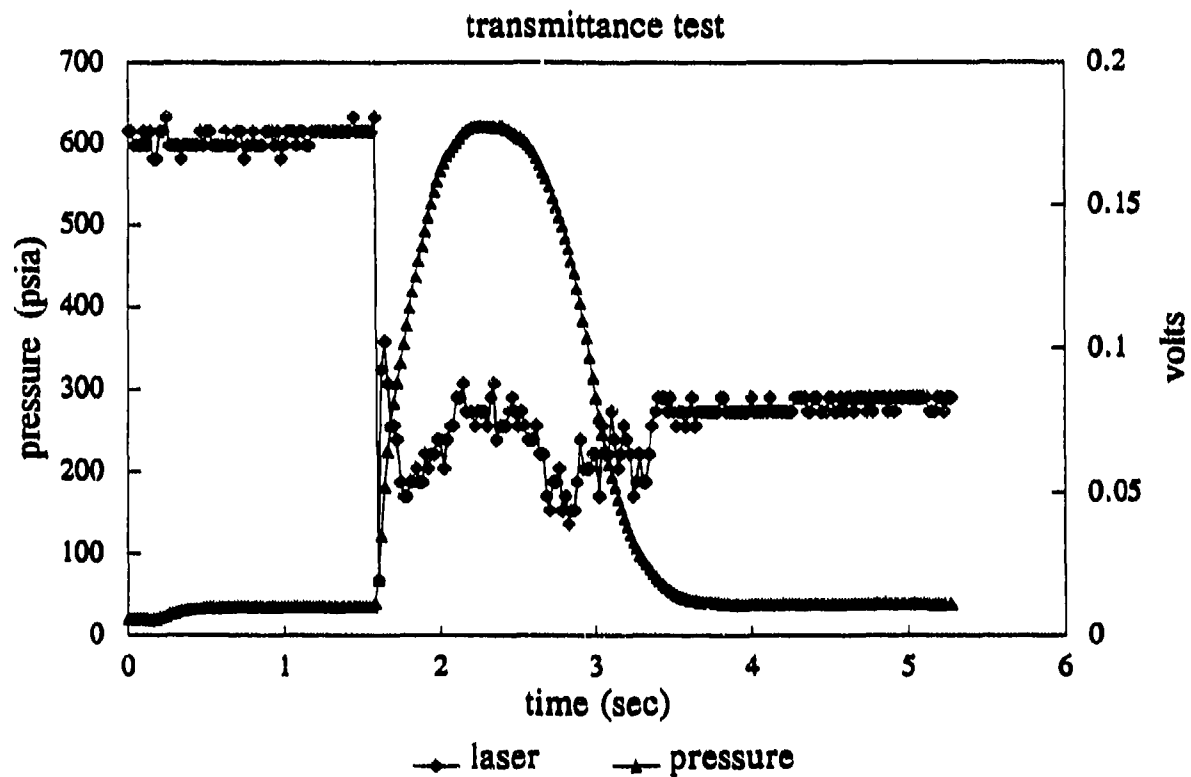
Figure 10. Transmittance Test Through Modified Motor

AC-7   5-31-94
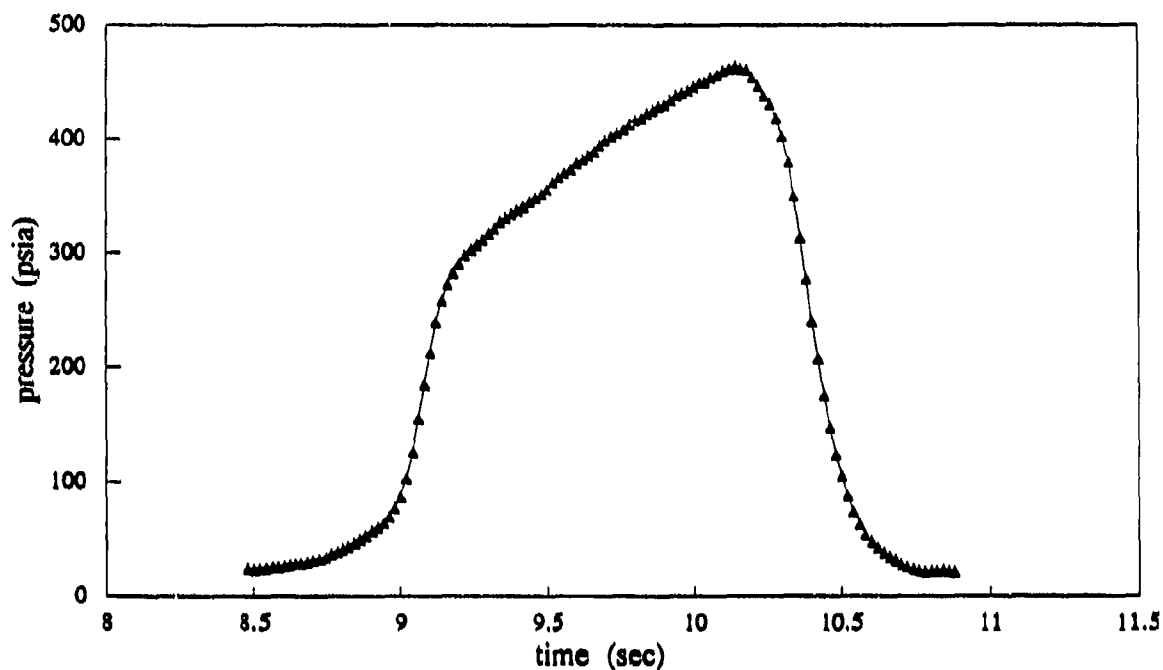
Figure 11. 18% Aluminum Propellant Pressure-Time Trace

AC-13   6-2-92
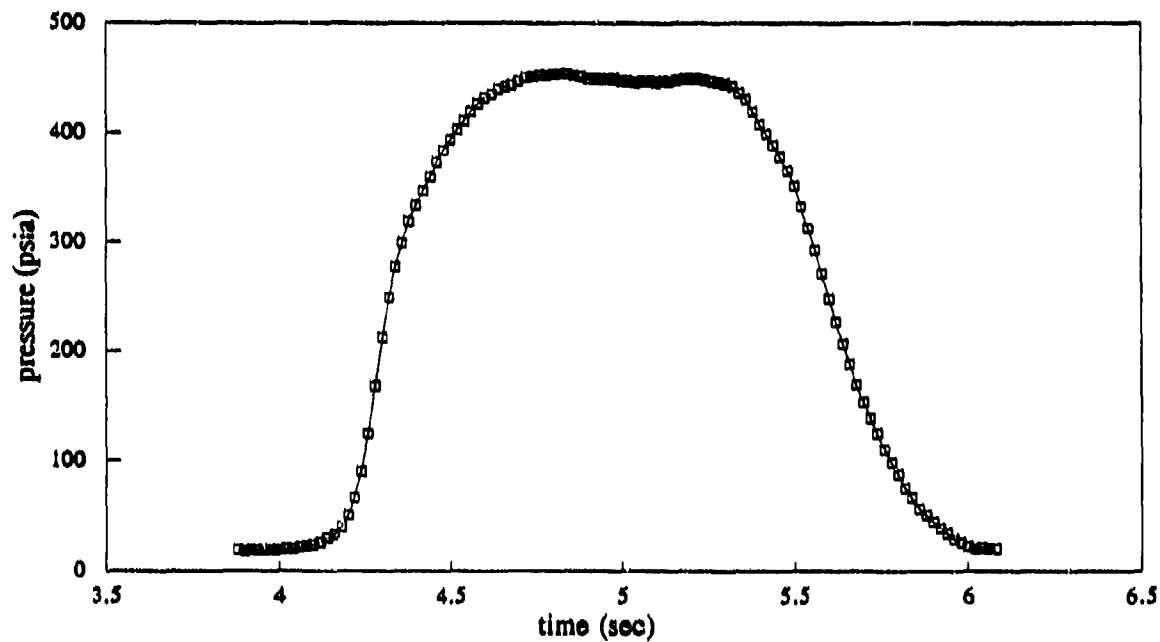
Figure 12. 13.5/4.5% Aluminum/Silicon Propellant Pressure-Time Trace

38

AC-14 6-4-94
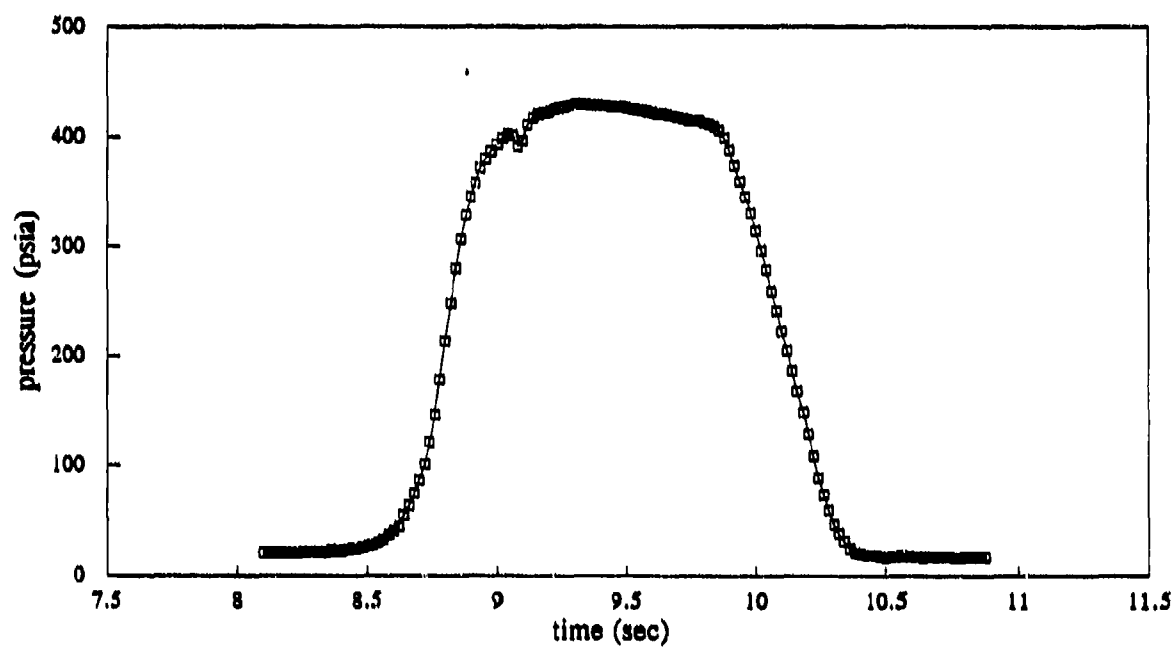
Figure 13. 12/6% Aluminum/Silicon Propellant Pressure-Time Trace

3 9
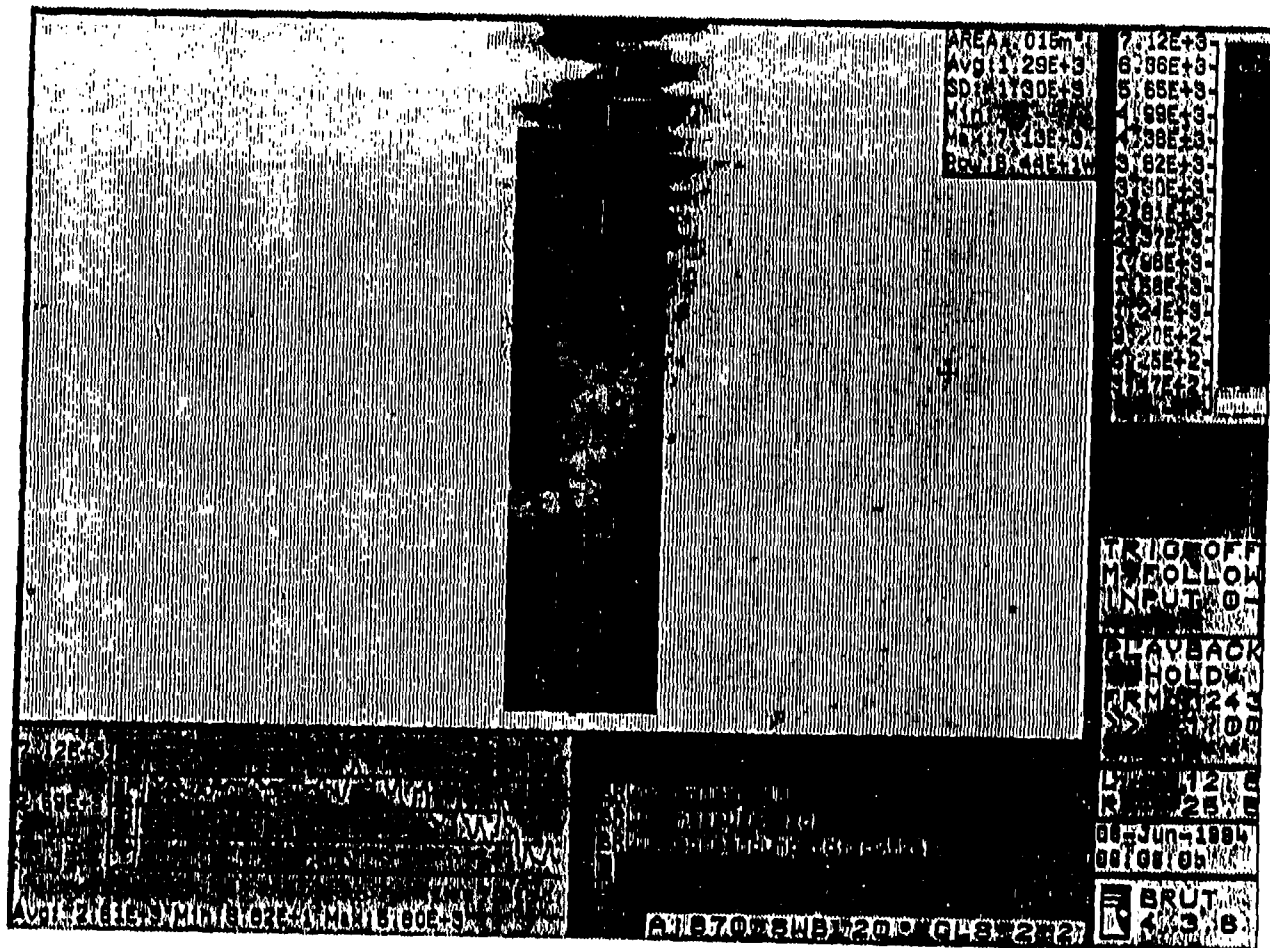
Figure 14. 18% Aluminum Propellant Thermal Image

Figure 15. 13.5/4.5% Aluminum/Silicon Propellant Thermal Image

Figure 16. 12/6% Aluminum/Silicon Propellant Thermal Image
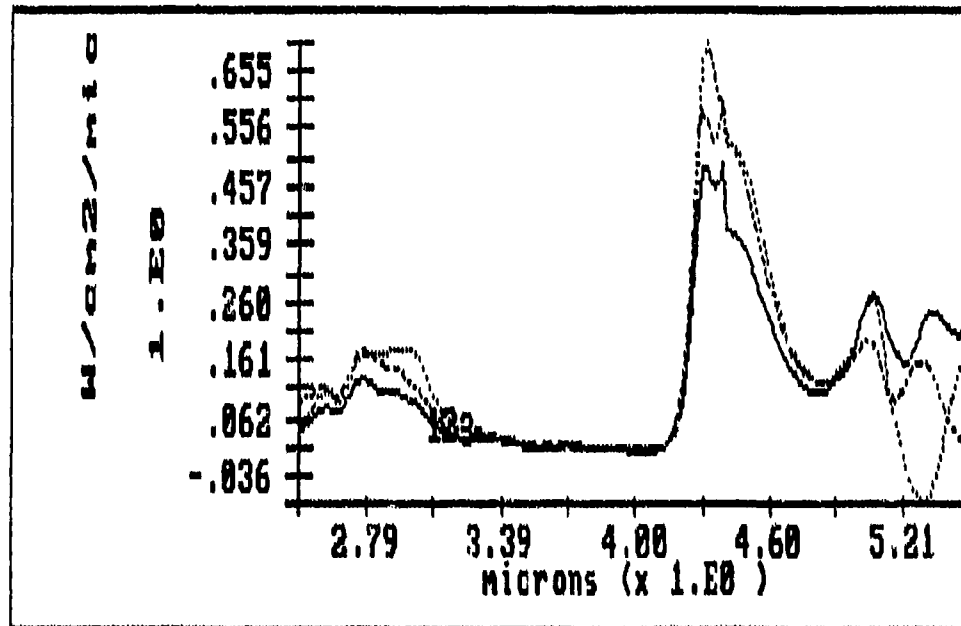
Figure 17. Propellant Plume Spectrum for all Three Propellants

43
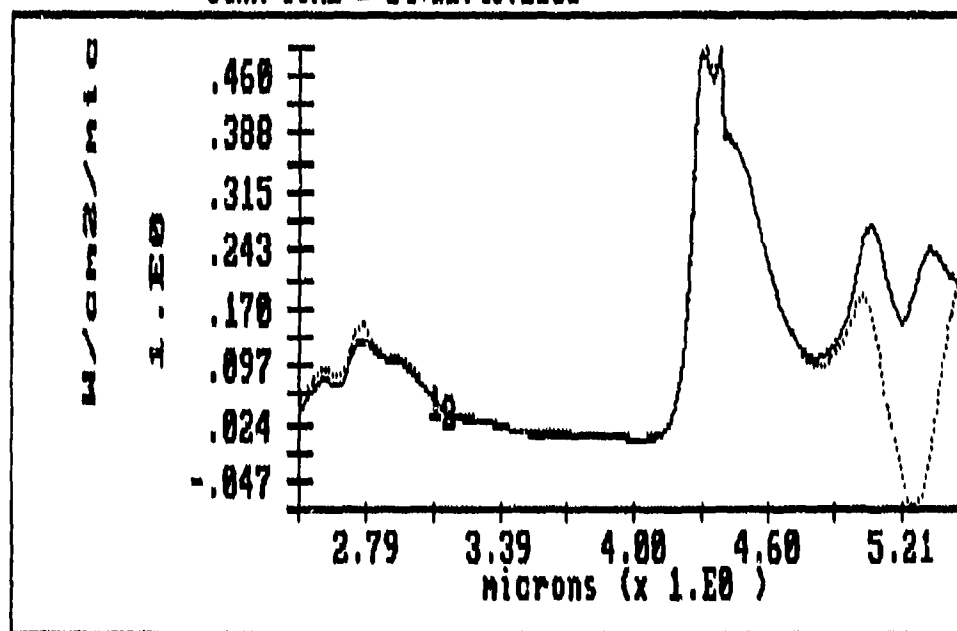
Figure 18. 18% Aluminum Propellant Spectrums at 400 and 450 psia

44

Upper	in	Lower	Under	Upper	in	Lower	Under	Upper	in	Lower	Under	Span
				57.7	0.0	49.8	100	9.82	0.0	8.47	100	1.20
				49.8	0.0	43.0	100	8.47	0.0	7.30	100	
				43.0	0.0	37.0	100	7.30	0.0	6.30	100	D[4,3]
				37.0	0.0	32.0	100	6.30	0.0	5.43	99.9	1.18µm
188	0.0	162	100	32.0	0.0	27.5	100	5.43	0.1	4.68	99.8	
162	0.0	140	100	27.5	0.0	23.8	100	4.68	0.2	4.05	99.7	D[3,2]
140	0.0	121	100	23.8	0.0	20.5	100	4.05	1.2	3.48	98.5	1.05µm
121	0.0	104	100	20.5	0.0	17.7	100	3.48	2.4	3.02	96.1	
104	0.0	89.8	100	17.7	0.0	15.3	100	3.02	2.9	2.60	93.2	D[v,0,9]
89.8	0.0	77.5	100	15.3	0.0	13.2	100	2.60	1.8	2.23	91.4	1.98µm
77.5	0.0	66.8	100	13.2	0.0	11.4	100	2.23	1.9	1.93	89.5	
66.8	0.0	57.7	100	11.4	0.0	9.82	100	1.93	89.5	0.50	0.0	D[v,0,1]
												0.67µm

Source = Data:Input	Beam length = 30.0 mm	Model indp [3, 0]	D[v,0,5]
	Log. Diff. = 2.899		1.09µm
Focal length = 100 mm	Obscuration = 0.6000	Volume Conc. = 0.0011%	
Presentation = pia	Volume distribution	Sp.S.A 5.8900 m²/cc.	Shape OFF

2048 pia ldr487 / 3/ 0/0.00/1.00/
AC-7 100 mm lens 30 sweeps small scrap stuck to back
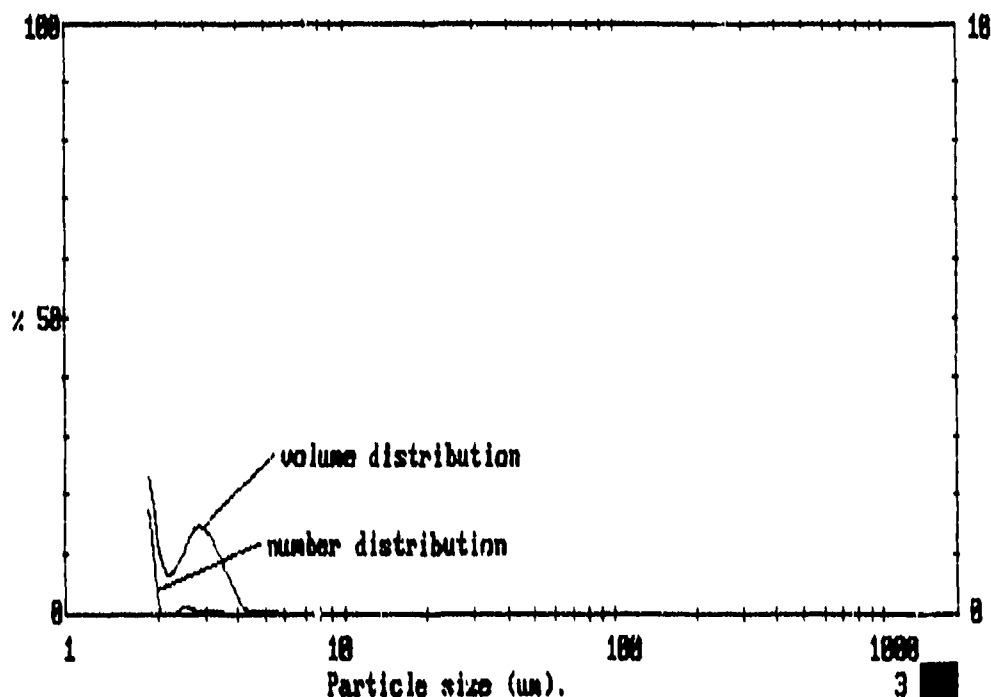
000001129

2048 pia ldr487 / 3/ 0/0.00/1.00/
AC-7 100 mm lens 30 sweeps small scrap stuck to back

000001129

Figure 19. Malvern Measurement: 18% Aluminum Propellant

45

Upper	in	Lower	Under	Upper	in	Lower	Under	Upper	in	Lower	Under	Span
				57.7	0.0	49.8	100	9.82	0.0	8.47	100	0.85
				49.8	0.0	43.0	100	8.47	0.0	7.30	100	
				43.0	0.0	37.0	100	7.30	0.0	6.30	100	D[4,3]
				37.0	0.0	32.0	100	6.30	0.0	5.43	100	0.98µm
188	0.0	162	100	32.0	0.0	27.5	100	5.43	0.0	4.68	100	
162	0.0	140	100	27.5	0.0	23.8	100	4.68	0.0	4.05	100	D[3,2]
140	0.0	121	100	23.8	0.0	20.5	100	4.05	0.0	3.48	100	0.98µm
121	0.0	104	100	20.5	0.0	17.7	100	3.48	0.0	3.02	100	
104	0.0	89.8	100	17.7	0.0	15.3	100	3.02	0.0	2.60	100	D[v,0.9]
89.8	0.0	77.5	100	15.3	0.0	13.2	100	2.60	0.0	2.23	100	1.50µm
77.5	0.0	66.8	100	13.2	0.0	11.4	100	2.23	0.0	1.93	100	
66.8	0.0	57.7	100	11.4	0.0	9.82	100	1.93	100	0.50	0.0	D[v,0.1] 0.65µm

Source = Data:Input	Beam length = 30.0 mm	Model indp [2, 0]	D[v,0.5]
	Log. Diff. = 4.278		0.99µm
Focal length = 100 mm	Obscuration = 0.7226	Volume Conc. = 0.0014%	
Presentation = pia	Volume distribution	Sp.S.A 6.1018 m²/cc.	Shape Off

```
2048  pia ldr487 / 2/ 0/0.00/1.00/
AC-13, small motor,thru plume, dthroat=.270", dexit=.50"
100 mm lens, 30 sweeps,starting at p=100psia          000001106 000001124
```

MALVERN   Series 2600   SB.0D   Master Mode   05 Jun 1994   11:32 am


```
2048  pia ldr487 / 2/ 0/0.00/1.00/
AC-13, small motor,thru plume, dthroat=.270", dexit=.50"
100 mm lens, 30 sweeps,starting at p=100psia          000001106 000001124
```

Figure 20. Malvern Measurement: 13.5/4.5% Aluminum/Silicon Propellant

Upper	in	Lower	Under	Upper	in	Lower	Under	Upper	in	Lower	Under	Span 0.85
				57.7	0.0	49.8	100	9.82	0.0	8.47	100	
				49.8	0.0	43.0	100	8.47	0.0	7.30	100	D[4,3] 0.98μm
				43.0	0.0	37.0	100	7.30	0.0	6.30	100	
				37.0	0.0	32.0	100	6.30	0.0	5.43	100	
188	0.0	162	100	32.0	0.0	27.5	100	5.43	0.0	4.68	100	D[3,2] 0.98μm
162	0.0	140	100	27.5	0.0	23.8	100	4.68	0.0	4.05	100	
140	0.0	121	100	23.8	0.0	20.5	100	4.05	0.0	3.48	100	
121	0.0	104	100	20.5	0.0	17.7	100	3.48	0.0	3.02	100	D[v,0.9] 1.50μm
104	0.0	89.8	100	17.7	0.0	15.3	100	3.02	0.0	2.60	100	
89.8	0.0	77.5	100	15.3	0.0	13.2	100	2.60	0.0	2.23	100	
77.5	0.0	66.8	100	13.2	0.0	11.4	100	2.23	0.0	1.93	100	D[v,0.1] 0.65μm
66.8	0.0	57.7	100	11.4	0.0	9.82	100	1.93	100	0.50	0.0	

Source = Data:Input	Beam length = 30.0 mm	Model indp [2, 0]	D[v,0.5] 0.99μm
	Log. Diff. = 4.040		
Focal length = 100 mm	Obscuration = 0.7279	Volume Conc. = 0.0014%	
Presentation = pia	Volume distribution	Sp.S.A 6.1018 m²/cc.	Shape OFF

2048 pia ldr487 / 2/ 0/0.00/1.00/
AC-14, small motor,thru plume, dthroat=.270", dexit=.50"
100 mm lens, 30 sweeps,starting at p=100psia   000001106 000001125

MALVERN   Series 2600   SB.0D   Master Mode   05 Jun 1994   11:36 am

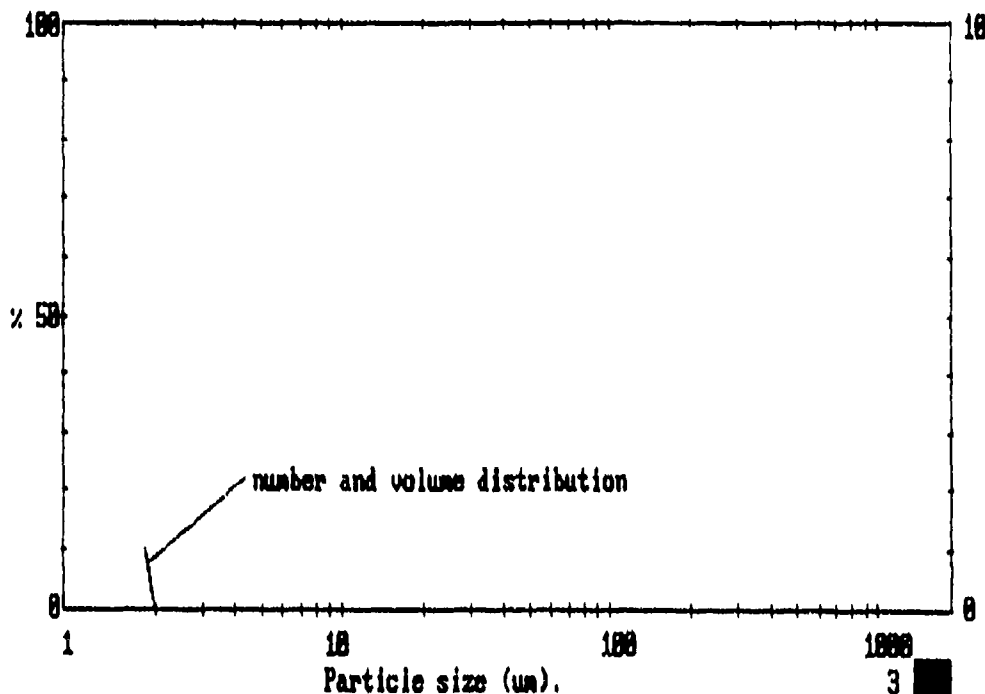number and volume distribution

% — Particle size (um).

2048 pia ldr487 / 2/ 0/0.00/1.00/
AC-14, small motor,thru plume, dthroat=.270", dexit=.50"
100 mm lens, 30 sweeps,starting at p=100psia   000001106 000001125
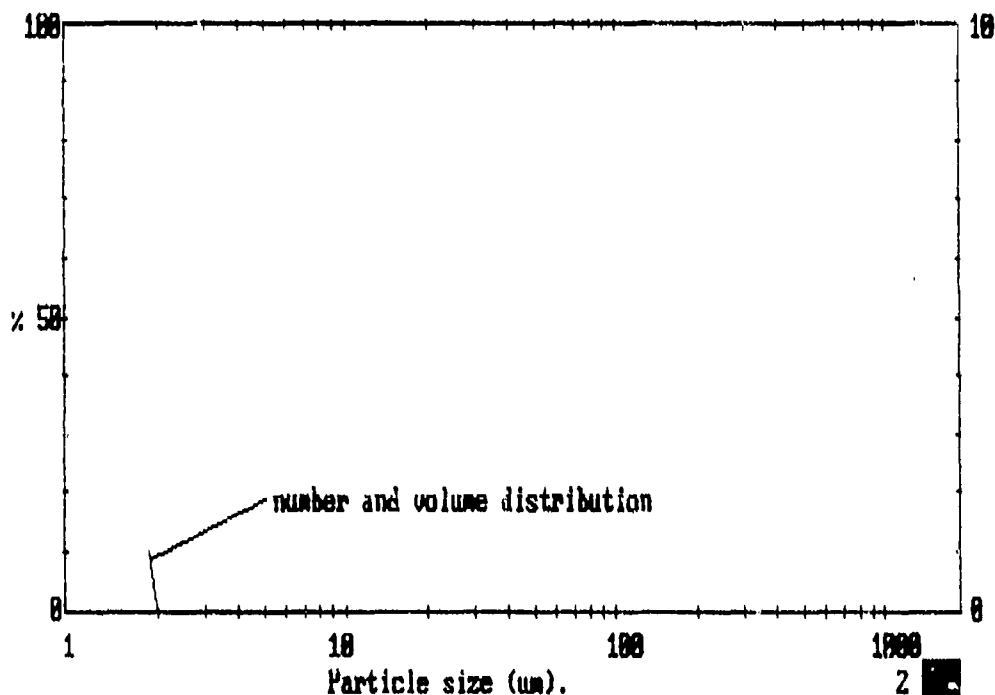
Figure 21. Malvern Measurement: 12/6% Aluminum/Silicon Propellant

APPENDIX B

MICROPEP EQUILIBRIUM COMPUTATIONS FOR RADIATION PROPELLANTS

* 18% Al   *

INGREDIENT	MASS (gm)	HF (kcal/kg)	DENSITY (kg,'m**3)	COMPOSITION			
R45M	10.14	-30.0	899.5969	667C	999H	50	
AMMONIUM PERCHLORATE (AP)	67.15	-602.0	1948.6650	1CL	4H	1N	40
DIOCTYL ADIPATE	3.91	-733.0	916.9728	42H	22C	40	
TRI-PHENYL BISMUTH	.02	255.0	1586.0590	18C	15H	1BI	
IPDI	.78	-501.0	1062.9080	12C	18H	2N	20
ALUMINUM (PURE CRYSTALINE)	18.00	.0	2701.5590	1AL			

VOLUME PERCENT OF INGREDIENTS (IN ORDER)

    19.6388   60.0389   7.4131   .0220   1.2786   11.6087

THE PROPELLANT DENSITY IS   .06294 LB/CU-IN OR   1.7423 GM/CC

THE EQUIVALENCE RATIO IS   1.7045

NUMBER OF GRAM ATOMS OF EACH ELEMENT PRESENT IN INGREDIENTS

    3.906379 H   1.018413 C   .578522 N   2.340811 O
    .667161 AL   .571504 CL   .000045 BI

************************************CHAMBER RESULTS FOLLOW********************************

TEMP (K)	PRESSURE (MPa/ATM/PSI)	ENTHALPY (kJ/kg)	ENTROPY (kJ/kg-K)	CP/CV	SGAMMA	Pi/ni (MPa/kmol)
3275.1	2.758/ 27.22/ 400.00	-1840.1320	9.842	1.1780	1.1341	75231.840

DAMPED AND UNDAMPED SPEED OF SOUND= 886.564 AND 1084.305 m/sec

SPECIFIC HEAT (MOLAR) OF GAS AND TOTAL=38766.540   50737.980 J/kmol-K
NUMBER MOLS GAS AND CONDENSED=   3.6659   .3097

(*=liquid,&=solid)

1.29702 H2	.98569 CO	.48472 HCl	.33279 H2O
.30965 Al2O3*	.28876 N2	.14341 H	.03583 Cl
.03260 CO2	.02991 AlCl	.01521 HO	.00679 AlCl2
5.39E-03 AlOCl	1.71E-03 AlHO	1.34E-03 AlHO2	9.89E-04 O
8.89E-04 NO	6.90E-04 Al	6.84E-04 AlO	6.54E-04 AlCl3
2.78E-04 Al2O	1.09E-04 AlH	1.00E-04 O2	6.18E-05 CHO
4.54E-05 Bi	4.39E-05 Cl2	3.54E-05 NH3	3.06E-05 CNH
2.12E-05 COCl	1.66E-05 Al2O2	1.39E-05 N	1.39E-05 NH2
8.26E-06 HOCl	8.01E-06 OCl	6.72E-06 NH	5.32E-06 CH2O
2.90E-06 AlO2	1.38E-06 AlHO	1.32E-06 CNHO	1.30E-06 NHO
9.63E-07 HO2	5.37E-07 CN	2.18E-07 CH3	9.17E-08 CNCl
9.02E-08 CH4	8.72E-08 CNO	7.52E-08 N2O	5.59E-08 NOCl
5.34E-08 CH2	2.23E-08 NO2	1.84E-08 Al2	1.58E-08 AlN
1.31E-08 CH	1.22E-08 C	5.27E-09 NHO2	4.98E-09 C2H2
4.97E-09 C2O	4.71E-09 NHO2		

THE MOLECULAR WEIGHT OF THE MIXTURE IS   25.154 gm/mole
THE GAS CONSTANT IS   330.54 J/kg-K

TOTAL HEAT CONTENT (298 REF)   =   5576.333 kJ/kg
SENSIBLE HEAT CONTENT (298 REF)=   5346.231 kJ/kg

```
*************************EXHAUST RESULTS FOLLOW*****************************

TEMP        PRESSURE            ENTHALPY   ENTROPY   CP/CV  SGAMMA    Pi/ni
(K)        (MPa/ATM/PSI)         (kJ/kg)   (kJ/kg-K)                 (MPa/kmol)
2327.1     .101/  1.00/  14.70  -4555.4170  9.842   1.1904  1.0000    2844.234

DAMPED AND UNDAMPED SPEED OF SOUND= 727.181 AND  905.884 m/sec

SPECIFIC HEAT (MOLAR) OF GAS AND TOTAL=37482.100   47537.910 J/kmol-K
NUMBER MOLS GAS AND CONDENSED=   3.5634    .3330

(*=liquid,&=solid)
  1.37301 H2          .98214 CO          .56271 HCl         .28925 N2
   .28606 H2O         .23203 Al2O3&      .10095 Al2O3*      .03627 CO2
  2.46E-02 H         7.22E-03 Cl        8.75E-04 HO        6.68E-04 AlCl
  2.36E-04 AlCl2     1.58E-04 AlOCl     9.20E-05 AlCl3     4.54E-05 Bi
  2.20E-05 NO        1.91E-05 AlHO      1.62E-05 AlHO2     1.04E-05 O
  3.16E-06 NH3       3.13E-06 Cl2       1.42E-06 CNH       1.24E-06 CHO
  9.19E-07 Al        9.09E-07 O2        7.94E-07 AlO       5.09E-07 COCl
  2.31E-07 CH2O      1.80E-07 NH2       1.41E-07 HOCl      8.63E-08 AlH
  5.63E-08 Al2O      5.30E-08 N         4.45E-08 OCl       4.01E-08 CNHO
  2.46E-08 NH        5.82E-09 NHO       4.73E-09 CH4

THE MOLECULAR WEIGHT OF THE MIXTURE IS   25.665 gm/mole
THE GAS CONSTANT IS   323.96 J/kg-K

TOTAL HEAT CONTENT (298 REF)    =   3479.104 kJ/kg
SENSIBLE HEAT CONTENT (298 REF)=    3347.614 kJ/kg

***************************************************************************

An exact method for determining throat conditions was used
The frozen & shifting STATE gammas for the throat are:  1.1766  1.1356
GAMMA NU shown below is the gamma for the chamber to throat PROCESS.

**********PERFORMANCE:  FROZEN ON FIRST LINE, SHIFTING ON SECOND LINE,*********
***************SHIFTING TO THROAT/FROZEN AFTERWARDS ON THIRD LINE*************

SPECIFIC GAMMA  T*     P*    C*     ISP*   Ae/A*  D-ISP    A*/m    Te    Cf
IMPULSE  NU                                      (gm-s/  (cm**2/
(sec)          (K)    (MPa) (m/s)  (sec)          cm**3)  kg/s)   (K)
232.0  1.1789 3006.  1.568 1550.4        4.623 11188.760  5.6212 1966. 1.4675
237.7  1.1355 3091.  1.592 1571.7 197.6  5.123 11460.990  5.6981 2327. 1.4830
234.1  1.1355 3091.  1.592 1571.7 197.6  4.628 11290.230  5.6981 2029. 1.4609

FROZEN & SHIFTING KINETIC ENERGY OF EXHAUST  518629.  636790.  m**2/s**2
```

* 13.5/4.5% Al/Si *

INGREDIENT	MASS (gm)	HF (kcal/kg)	DENSITY (kg/m**3)	COMPOSITION			
R45M	10.14	-30.0	899.5969	667C	999H	50	
AMMONIUM PERCHLORATE (AP)	67.15	-602.0	1948.6650	1CL	4H	1N	40
DIOCTYL ADIPATE	3.91	-733.0	918.9728	42H	22C	40	
TRI-PHENYL BISMUTH	.02	255.0	1586.0590	18C	15H	1BI	
IPDI	.78	-501.0	1062.9080	12C	18H	2N	20
ALUMINUM (PURE CRYSTALINE)	13.50	.0	2701.5590	1AL			
SILICON (PURE CRYSTALINE)	4.50	.0	2419.2240	1SI			

VOLUME PERCENT OF INGREDIENTS (IN ORDER)

```
   19.5725     59.8363      7.3881       .0219      1.2742      8.6771
    3.2299
```

THE PROPELLANT DENSITY IS .06273 LB/CU-IN OR 1.7364 GM/CC

THE EQUIVALENCE RATIO IS   1.7045

NUMBER OF GRAM ATOMS OF EACH ELEMENT PRESENT IN INGREDIENTS

```
    3.906379 H     1.018413 C       .578522 N      2.340811 O
     .500371 AL      .160199 SI      .571504 CL      .000045 BI
```

*************************CHAMBER RESULTS FOLLOW***************************

TEMP (K)	PRESSURE (MPa/ATM/PSI)	ENTHALPY (kJ/kg)	ENTROPY (kJ/kg-K)	CP/CV	SGAMMA	Pi/ni (MPa/kmol)
3045.6	2.758/ 27.22/ 400.00	-1840.1320	9.830	1.1930	1.1544	73229.410

DAMPED AND UNDAMPED SPEED OF SOUND= 918.869 AND 1066.569 m/sec

SPECIFIC HEAT (MOLAR) OF GAS AND TOTAL=39027.600 48286.560 J/kmol-K
NUMBER MOLS GAS AND CONDENSED= 3.7661   .2419

(*=liquid,&=solid)

1.26248 H2	.97803 CO	.52976 HCl	.38322 H2O
.28901 N2	.24186 Al2O3*	.15951 SiO	.07586 H
.04030 CO2	.02155 Cl	.00931 AlCl	.00811 HO
3.31E-03 AlCl2	2.16E-03 AlOCl	5.94E-04 AlCl3	5.61E-04 SiO2
5.20E-04 AlHO	5.05E-04 AlHO2	4.13E-04 NO	2.93E-04 O
1.04E-04 SiCl2	1.04E-04 AlO	8.80E-05 Al	4.54E-05 Bi
3.89E-05 CHO	3.79E-05 NH3	3.55E-05 O2	3.15E-05 Cl2
2.44E-05 CNH	2.38E-05 Al2O	1.65E-05 AlH	1.52E-05 COCl
1.16E-05 SiCl	8.66E-06 Si	7.98E-06 NH2	5.08E-06 HOCl
5.05E-06 CH2O	3.71E-06 N	3.49E-06 SiH	3.05E-06 OCl
2.86E-06 SiCl3	2.34E-06 NH	1.63E-06 Al2O2	1.20E-06 CNHO
6.44E-07 SiN	5.77E-07 NHO	3.92E-07 AlO2	3.33E-07 HO2
2.26E-07 AlHO	1.94E-07 CN	1.66E-07 CH3	1.23E-07 CH4
1.15E-07 SiHCl3	9.90E-08 SiH2Cl2	6.07E-08 CNCl	3.88E-08 CNO
3.41E-08 N2O	3.17E-08 SiCl4	2.89E-08 SiH3Cl	2.37E-08 NOCl
2.15E-08 CH2	7.12E-09 NO2		

THE MOLECULAR WEIGHT OF THE MIXTURE IS   24.950 gm/mole
THE GAS CONSTANT IS   333.24 J/kg-K

TOTAL HEAT CONTENT (298 REF)   =   4942.663 kJ/kg
SENSIBLE HEAT CONTENT (298 REF)=   4728.822 kJ/kg

*********************EXHAUST RESULTS FOLLOW***************************

TEMP (K)	PRESSURE (MPa/ATM/PSI)	ENTHALPY (kJ/kg)	ENTROPY (kJ/kg-K)	CP/CV	SGAMMA	Pi/ni (MPa/kmol)
2294.0	.101/ 1.00/ 14.70	-4465.3200	9.830	1.2012	1.1301	2823.397

DAMPED AND UNDAMPED SPEED OF SOUND= 732.198 AND 906.821 m/sec

SPECIFIC HEAT (MOLAR) OF GAS AND TOTAL=37215.790 48046.910 J/kmol-K
NUMBER MOLS GAS AND CONDENSED=   3.5898   .1183

(*=liquid,&=solid)
1.41073 H2	.98690 CO	.56394 HCl	.28925 N2
.24961 H2O	.06567 Al6Si2Ol	.05265 Al2O3&	.03151 CO2
2.88E-02 SiO	2.11E-02 H	6.06E-03 Cl	6.10E-04 HO
5.97E-04 AlCl	2.29E-04 AlCl2	1.23E-04 AlOCl	1.02E-04 AlCl3
4.54E-05 Bi	2.78E-05 SiO2	1.46E-05 AlHO	1.45E-05 NO
1.07E-05 AlHO2	6.39E-06 SiCl2	6.12E-06 O	3.40E-06 NH3
2.65E-06 Cl2	1.69E-06 CNH	1.12E-06 CHO	6.72E-07 Al
4.97E-07 AlO	4.54E-07 O2	4.51E-07 COCl	2.39E-07 CH2O
1.61E-07 NH2	1.50E-07 SiCl3	1.10E-07 SiCl	9.81E-08 HOCl
6.73E-08 AlH	5.11E-08 Si	4.02E-08 CNHO	3.83E-08 Al2O
3.72E-08 N	2.68E-08 OCl	1.88E-08 NH	1.19E-08 SiH
6.87E-09 CH4			

THE MOLECULAR WEIGHT OF THE MIXTURE IS   26.968 gm/mole
THE GAS CONSTANT IS   308.30 J/kg-K

TOTAL HEAT CONTENT (298 REF)   =   3325.127 kJ/kg
SENSIBLE HEAT CONTENT (298 REF)=   3211.227 kJ/kg

****

An exact method for determining throat conditions was used
The frozen & shifting STATE gammas for the throat are: 1.1928   1.1607
GAMMA NU shown below is the gamma for the chamber to throat PROCESS.

**********PERFORMANCE: FROZEN ON FIRST LINE, SHIFTING ON SECOND LINE,*********
***************SHIFTING TO THROAT/FROZEN AFTERWARDS ON THIRD LINE**************

SPECIFIC IMPULSE (sec)	GAMMA NU	T* (K)	P* (MPa)	C* (m/s)	ISP* (sec)	Ae/A*	D-ISP (gm-s/ cm**3)	A*/m (cm**2/ kg/s)	Te (K)	Cf
224.9	1.1943	2776.	1.559	1508.3		4.507	10807.170	5.4684	1759.	1.4620
233.7	1.1580	2838.	1.578	1525.2	192.3	5.331	11231.190	5.5295	2294.	1.5026
226.5	1.1580	2838.	1.578	1525.2	192.3	4.510	10886.910	5.5295	1803.	1.4565

FROZEN & SHIFTING KINETIC ENERGY OF EXHAUST 468477. 643975. m**2/s**2

52

* 12/6% Al/Si   *

INGREDIENT	MASS (gm)	HF (kcal/kg)	DENSITY (kg/m**3)	COMPOSITION			
R45M	10.14	-30.0	899.5969	667C	999H	5O	
AMMONIUM PERCHLORATE (AP)	67.15	-602.0	1948.6650	1CL	4H	1N	4O
DIOCTYL ADIPATE	3.91	-733.0	918.9728	42H	22C	4O	
TRI-PHENYL BISMUTH	.02	255.0	1586.0590	18C	15H	1BI	
IPDI	.78	-501.0	1062.9080	12C	18H	2N	2O
ALUMINUM (PURE CRYSTALINE)	12.00	.0	2701.5590	1AL			
SILICON (PURE CRYSTALINE)	6.00	.0	2419.2240	1SI			

VOLUME PERCENT OF INGREDIENTS (IN ORDER)

    19.5505   59.7690   7.3797   .0219   1.2728   7.7043
     4.3017

THE PROPELLANT DENSITY IS .06266 LB/CU-IN OR 1.7345 GM/CC

THE EQUIVALENCE RATIO IS   1.7045

NUMBER OF GRAM ATOMS OF EACH ELEMENT PRESENT IN INGREDIENTS

    3.906379 H   1.018413 C   .578522 N   2.340811 O
     .444774 AL   .213599 SI   .571504 CL   .000045 BI

**************************CHAMBER RESULTS FOLLOW*****************************

TEMP (K)	PRESSURE (MPa/ATM/PSI)	ENTHALPY (kJ/kg)	ENTROPY (kJ/kg-K)	CP/CV	SGAMMA	Pi/ni (MPa/kmol)
2951.7	2.758/ 27.22/ 400.00	-1840.1320	9.816	1.1991	1.1640	72507.210

DAMPED AND UNDAMPED SPEED OF SOUND= 927.693 AND 1057.879 m/sec

SPECIFIC HEAT (MOLAR) OF GAS AND TOTAL=39088.090 47373.030 J/kmol-K
NUMBER MOLS GAS AND CONDENSED= 3.8036   .2172

(*=liquid,&=solid)

1.24689 H2	.97443 CO	.54124 HCl	.40388 H2O
.28908 N2	.21719 Al2O3*	.21267 SiO	.05676 H
.04391 CO2	.01677 Cl	.00601 HO	.00541 AlCl
2.32E-03 AlCl2	1.39E-03 AlOCl	7.40E-04 SiO2	5.43E-04 AlCl3
3.20E-04 AlHO2	3.01E-04 AlHO	2.88E-04 NO	1.66E-04 O
1.60E-04 SiCl2	4.54E-05 Bi	4.38E-05 AlO	3.93E-05 NH3
3.47E-05 Al	3.16E-05 CHO	2.61E-05 Cl2	2.23E-05 CNH
2.16E-05 O2	1.29E-05 COCl	1.24E-05 SiCl	7.80E-06 Al2O
7.35E-06 Si	7.06E-06 AlH	6.21E-06 NH2	5.15E-06 SiCl3
4.95E-06 CH2O	3.95E-06 HOCl	3.24E-06 SiH	2.04E-06 N
1.91E-06 OCl	1.45E-06 NH	1.15E-06 CNHO	5.99E-07 SiN
5.64E-07 Al2O2	3.94E-07 NHO	2.31E-07 SiHCl3	2.01E-07 HO2
1.75E-07 SiH2Cl2	1.56E-07 AlO2	1.50E-07 CH3	1.45E-07 CH4
1.24E-07 CN	9.86E-08 AlHO	7.14E-08 SiCl4	5.02E-08 CNCl
4.47E-08 SiH3Cl	2.69E-08 CNO	2.35E-08 N2O	1.56E-08 NOCl
1.44E-08 CH2			

THE MOLECULAR WEIGHT OF THE MIXTURE IS   24.871 gm/mole
THE GAS CONSTANT IS   334.30 J/kg-K

```
TOTAL HEAT CONTENT (298 REF)   =   4705.487 kJ/kg
SENSIBLE HEAT CONTENT (298 REF)=   4493.867 kJ/kg


*****************************EXHAUST RESULTS FOLLOW*****************************

TEMP       PRESSURE          ENTHALPY   ENTROPY   CP/CV   SGAMMA    Pi/ni
(K)       (MPa/ATM/PSI)      (kJ/kg)   (kJ/kg-K)                   (MPa/kmol)
2243.9    .101/  1.00/  14.70  -4449.4190   9.816   1.2032   1.1202   2813.930


DAMPED AND UNDAMPED SPEED OF SOUND= 729.060 AND  899.133 m/sec

SPECIFIC HEAT (MOLAR) OF GAS AND TOTAL=37087.180   47954.760 J/kmol-K
NUMBER MOLS GAS AND CONDENSED=   3.6018    .0952

(*=liquid,&=solid)
   1.42033 H2           .98724 CO           .56604 HCl           .28925 N2
    .24148 H2O          .07404 Al6Si2O1     .04431 SiO           .03117 CO2
   2.11E-02 SiO2*      1.63E-02 H          4.68E-03 Cl          4.20E-04 HO
   2.64E-04 AlCl       1.18E-04 AlCl2      6.60E-05 AlCl3       5.45E-05 AlOCl
   4.54E-05 Bi         3.84E-05 SiO2       1.18E-05 SiCl2       9.37E-06 NO
   6.04E-06 AlHO       4.34E-06 AlHO2      3.64E-06 NH3         3.26E-06 O
   2.12E-06 Cl2        1.76E-06 CNH        9.39E-07 CHO         3.80E-07 COCl
   3.16E-07 SiCl3      2.42E-07 CH2O       2.33E-07 O2          2.12E-07 Al
   1.53E-07 AlO        1.49E-07 SiCl       1.30E-07 NH2         6.91E-08 HOCl
   5.72E-08 Si         3.96E-08 CNHO       2.31E-08 AlH         2.12E-08 N
   1.52E-08 OCl        1.47E-08 SiH        1.22E-08 NH          1.06E-08 SiHCl3
   9.36E-09 CH4        7.00E-09 SiCl4      6.94E-09 Al2O

THE MOLECULAR WEIGHT OF THE MIXTURE IS   27.049 gm/mole
THE GAS CONSTANT IS   307.38 J/kg-K

TOTAL HEAT CONTENT (298 REF)   =   3224.611 kJ/kg
SENSIBLE HEAT CONTENT (298 REF)=   3115.341 kJ/kg


******************************************************************************

An exact method for determining throat conditions was used
The frozen & shifting STATE gammas for the throat are:  1.1994  1.1718
GAMMA NU shown below is the gamma for the chamber to throat PROCESS.

**********PERFORMANCE:  FROZEN ON FIRST LINE, SHIFTING ON SECOND LINE,*********
***************SHIFTING TO THROAT/FROZEN AFTERWARDS ON THIRD LINE**************

SPECIFIC GAMMA   T*    P*    C*      ISP*   Ae/A*   D-ISP    A*/m    Te    Cf
IMPULSE   NU                                       (gm-s/  (cm**2/
(sec)           (K)   (MPa) (m/s)   (sec)          cm**3)   kg/s)  (K)
221.7   1.2003 2683. 1.556 1489.7          4.461  10644.090 5.4008 1679. 1.4596
233.0   1.1680 2740. 1.596 1504.5 189.9    5.321  11184.540 5.4544 2244. 1.5186
223.1   1.1680 2740. 1.596 1504.5 189.9    4.461  10711.100 5.4544 1714. 1.4544

FROZEN & SHIFTING KINETIC ENERGY OF EXHAUST  448358.  632859.  m**2/s**2
```

54

REFERENCES

1. Sutton, George P. *Rocket Propulsion Elements*, Sixth Edition, John Wiley & Sons, Inc., 1992, p 417.

2. Reed, R.A., Calia, V.S., *Review of Aluminum Oxide Rocket Exhaust Particles*, AIAA 28th Thermalphysics Conference, Jul. 6-9, 1993, Orlando FL.

3. Konopka, W.L., Reed, R.A., and Calia, V.S., *Measurements of Infrared Optical Properties of Al₂O₃ Rocket Particles*, Progress in Astronautics and Aeronautics: Spacecraft Radiance Transfer and Temperature Control, Vol. 83, edited by Horton, T.E., AIAA, New York, 1982, pp. 181-196.

4. Pluchino, A.B. *Emissivity Spectra of Composite Microscopic Particles*, Applied Optics, Vol. 20, No. 4, 15 Feb. 1981, pp. 531-533.

5. Pluchino, A.B., Masturzo, D.E., *Emissivity of Al₂O₃ Particles in a Rocket Plume*, AIAA Journal, Vol. 19, No. 9, Sept. 1981, pp. 1234-1237.

6. Grynak, D.A., Burch, D.E., *Optical and Infrared Properties of Al₂O₃ at Elevated Temperatures*, Journal of the Optical Society of America, Vol. 55, No. 6, pp. 625-629, June 1965.

7. Cruise, D.R., *Theoretical Computations of Equilibrium Compositions, Thermodyanamic Properties, and Performance Characteristics of Propellant Systems*, Naval Weapons Center, NWC TP 6037 Apr. 1979.

8. Hwang, C.J., and Chang, G.C., *Numerical Study of Gas-Particle Flow in a Solid Rocket Nozzle*, AIAA Journal, Vol. 26, No. 6, June 1988, pp. 682-689.

9. Netzer, D.W., Larado, D., et al, *Plume Particle Size Distribution and Optical Properties*, 20th JANNAF Exhaust Plume Technology Subcommittee Meeting, Vol. II, Feb., 1993, pp. 407-427.

10. Dill, K.M., Reed, R.A., Calia, V.S., and Schultz, R.J., *Analysis of Crystalline Phase Aluminum Oxide Particles from Solid Propellant Exhausts*, Journal of Propulsion, Vol. No. 5, Sept.-Oct. 1990, pp. 668-671.

11. Larado, D., McCrorie J. D., Netzer, D.W., Vaughn, J.K, *Motor and Plume Particle Size Measurements in Solid Propellant Micromotors*, Journal of Propulsion and Power, Vol. 10, No. 3 May-June 1994, pp410-418.

12. Gomes, P.V., *Validation and Implementation of Optical Diagnostics for Particle Sizing in Rocket Motors*, M.S.A.E. Thesis, Naval Postgraduate School, Monterey, CA., Dec. 1993.

13. Malvern System 2600, Instruction Manual, Malvern Systems Ltd.

14. SR 5000 Spectroradiometer, Instruction Manual, CI Systems, 1988.

15. Thermovision 870 Operating Manual, AGEMA Infrared Systems AB., 1986.

16. Aerometrics Laser Doppler Velocimeter Doppler Signal Analyzer, Component User's Manual, Release 1.0, April 1993.

17. Cashdollar, K.L., Lee, C.K., Singer, J.M., *Three-Wavelength Light Transmission Technique to Measure Smoke Particle Size and Concentration*, Applied Optics, Vol. 18, No. 11, June 1979, pp. 1763-1769.

INITIAL DISTRIBUTION LIST

		No. Copies
1.	Defense Technical Information Center Cameron Station Alexandria, Virginia 22304-6145	2
2.	Library, Code 52 Naval Postgraduate School Monterey, California 93943-5100	2
3.	Department Chairman, Code AA Department of Aeronautics Naval Postgraduate School Monterey, California 93943-5000	1
4.	Professor D.W. Netzer, Code AA/Nt Department of Aeronautics Naval Postgraduate School Monterey, California 93943-5000	2
5.	Professor C. F. Newberry Code AA/Ne Department of Aeronautics Naval Postgraduate School Monterey, California 93943-5000	1
6.	LCDR Clay J. Snaza 3504 Kings Road S. St. Augustine, Florida 32086	2